5G PPP

European Commission | Horizon 2020 European Union funding for Research & Innovation

5G-XHaul

Dynamically Reconfigurable Optical-Wireless Backhaul/Fronthaul with Cognitive Control Plane for Small Cells and Cloud-RANs

D4.3 Use of mm-Wave technology for backhaul, fronthaul and access networks

This project has received funding from the European Union's Framework Programme Horizon 2020 for research, technological development and demonstration

Advanced 5G Network Infrastructure for the Future Internet

Project Start Date: July 1st, 2015 Duration: 36 months

H2020-ICT-2014-2 671551 October 31st 2017 – Version 1.0

Project co-funded by the European Commission

Under the H2020 programme

Dissemination Level: **Confidential**

Grant Agreement Number:	671551
Project Name:	Dynamically Reconfigurable Optical-Wireless Back-haul/Fronthaul with Cognitive Control Plane for Small Cells and Cloud-RANs
Project Acronym:	5G-XHaul
Document Number:	D4.3
Document Title:	Use of mm-Wave technology for backhaul, fron-thaul and access networks
Version:	1.0
Delivery Date:	October 31st, 2017
Responsible:	Blu Wireless Technology (**BWT**)
Editor(s):	Peter Legg (**BWT**)
Authors:	Peter Legg (**BWT**), Jens Bartelt (**TUD**), Najeeb Ul Hassan (**HWDU**), Wen Xu (**HWDU**)
Keywords:	Millimetre wave, mesh, fronthaul, backhaul.
Status:	Final
Dissemination Level	Confidential
Project URL:	http://www.5g-xhaul-project.eu/

Version History

Rev. N	Description	Author	Date
0.90	First complete draft	Peter Legg (**BWT**)	10/10/2017
0.91	Updated Figure 3.5	Peter Legg (**BWT**)	11/10/2017
0.92	Updated after review by **UNIVBRIS**	Peter Legg (**BWT**)	20/10/2017
0.93	Updated after review by IHP	Peter Legg (**BWT**)	23/10/2017
1.0	Final review before submission	Jesús Gutiérrez (**IHP**)	31/10/2017

Table of Contents

EXECUTIVE SUMMARY **8**

1 INTRODUCTION **9**

2 MILLIMETRE WAVE FOR FRONTHAUL **10**

2.1 Performance of mmWave FH Technologies vs. FH Requirements **10**

3 JOINT DESIGN OF ACCESS AND FRONTHAUL/BACKHAUL **15**

3.1 Joint Design of Access and Fronthaul **15**

3.2 Wireless Self-backhauling **17**

3.2.1 Redundant Connectivity 17

3.2.2 Autonomous Configuration and Topology Adaptation 18

3.2.3 Multi-hop BH links 18

3.2.4 Flexible Resource Partitioning 18

4 MILLIMETRE WAVE MESHED BACKHAUL **20**

4.1 Single channel (reuse 1) performance assessment **22**

4.2 Multiple channel (reuse 3) performance assessment **26**

4.3 Single POP performance assessment **30**

5 SUMMARY AND CONCLUSIONS **36**

6 REFERENCES **37**

7 ACRONYMS **39**

List of Figures

Figure 1-1: Sketch on the technical work belonging to WP4. 9

Figure 2-1. Performance trade-offs for an IEEE 802.11ad PBSS with a unidirectional link with rate of 4.62 Gbps (MCS 12). 10

Figure 2-2: mmWave technology throughput performance vs. FH peak data rate requirements. 11

Figure 2-3: mmWave technology throughput performance vs. FH aggregate data rate requirements. 12

Figure 2-4: mmWave technology latency vs. FH requirements. 13

Figure 2-5. Delay between MACs plus a switching time of 0.3 ms for a bidirectional IEEE 802.11ad link loaded with 1800 Mbps of traffic in each direction 14

Figure 3-1: Principle of joint radio access and FH receiver. 16

Figure 3-2: Single-link BER performance of joint radio access and FH receiver compared to traditional receivers. 16

Figure 3-3: Throughput comparison of joint and conventional receiver for different scenarios [17]. 17

Figure 3-4 Example scenario with self-backhauling. 18

Figure 3-5: Possibilities for resource sharing between access and BH. 19

Figure 4-1. Cellular deployment under study. 20

Figure 4-2. Interference from overshoot of radiation when nodes are co-linear. 22

Figure 4-3. Network design of IEEE 802.11ad modems assigned to PBSSs (reuse 1, 3 POPs). 22

Figure 4-4. Network link chosen by the routing algorithm (reuse 1, 3 POPs). 23

Figure 4-5. Impact of interference (reuse 1, 3 POPs). 24

Figure 4-6. Hop count (reuse 1, 3 POPs). 24

Figure 4-7. Comparison of link rate CDFs with and without power control. 25

Figure 4-8. Throughput per node (reuse1, 3 POPs). 25

Figure 4-9. Mean latency per node (reuse1, 3 POPs). 26

Figure 4-10. Max latency per node (reuse1, 3 POPs). 26

Figure 4-11. Network design of IEEE 802.11ad modems assigned to PBSSs showing colouring /channel assignment (reuse 3, 3 POPs). 27

Figure 4-12. Network design of IEEE 802.11ad modems assigned to PBSSs (reuse 3, 3 POPs). 27

Figure 4-13. Impact of interference (reuse 3, 3 POPs). 28

Figure 4-14. Throughput per node (reuse3, 3 POPs). 29

Figure 4-15. Mean latency per node (reuse3, 3 POPs). 29

Figure 4-16. Max latency per node (reuse3, 3 POPs). 30

Figure 4-17. Network design of IEEE 802.11ad modems assigned to PBSSs showing colouring /channel assignment (reuse 3, 1 POP). 30

Figure 4-18. Network design of IEEE 802.11ad modems assigned to PBSSs (reuse 3, 1 POP). 31

Figure 4-19. Network link chosen by the routing algorithm (reuse 3, 1 POP). 31

Figure 4-20. Hop count (reuse3 1 POP). 32

Figure 4-21. SNR and SINR of routable links (reuse3 1 POP). 32

Figure 4-22. Throughput per node (reuse3, 1 POP). 33

Figure 4-23. Mean latency per node (reuse3, 1 POP). 33
Figure 4-24. Max latency per node (reuse3, 1 POP). 34
Figure 4-25. Comparative traffic load per node for dynamic simulations. 34
Figure 4-26. Mean (mean latency per pkt per node) in ms. 35

List of Tables

Table 2-1: Maximum data rates of 60 GHz IEEE 802.11 technologies. 11
Table 4-1. Simulator features. 21

Executive Summary

5G-XHaul focuses on developing a converged optical and wireless network solution supported by a flexible and scalable control plane with the aim to form a flexible transport infrastructure. This infrastructure will be able to jointly support the backhaul (BH) and fronthaul (FH) functionalities required to cope with the future challenges imposed by fifth generation (5G) Radio Access Networks (RANs).

In this context, one of the main topics of interest of 5G-XHaul is millimetre wave (mmWave) communications, both from the theoretical and simulation, to the implementation, integration and test. This work has been directed to analyse and study the use of mmWave in access, FH and BH.

The first contribution is an assessment of the viability of IEEE 802.11ad and IEEE 802.11ay mmWave technologies to provide wireless FH. Consideration is made with respect to the offered bandwidth and the latency. The conclusion is dependent on:

a) The number of bonded channel and MIMO streams of the IEEE 802.11ad/ay link.
b) The data rate of the remote radio unit (RRU) being fronthauled.
c) The functional split between RRU and CU (centralised unit).

Considering high performance 5G small cells it is recommended that a high functional split be used to bring the bandwidth and latency requirements into the capability range of a typical mmWave link.

The second piece of work considers firstly, a joint access and FH link, and secondly, the sharing of a radio channel between access and BH in the mmWave band.

Finally, there is a study on mmWave meshed BH using a dynamic system simulator. This demonstrates the viability of the technology over multiple-hops (up to four in the example studied), and shows the influence of the number of points of presence (POPs) and the number of radio channels available. The latency of the BH is approximately 0.5 ms per hop.

1 Introduction

One of the main technologies the 5G-XHaul project is currently tackling is the so-called millimetre wave (mmWave). Up to now, different partners of the consortium have focused their efforts in the research and development of mmWave systems and circuits.

The general architecture of the 5G-XHaul transport infrastructure data plane was firstly included in deliverable D2.2 [12] where, specifically, the wireless mmWave architecture was initially defined. Following this, there has been additional technical work in the context of Work Package (WP) 4. Figure 1-1 sketches the structure of the two main tasks which study mmWave aspects. Task 4.2.1 focuses on the research towards understanding the general mmWave-related research, and on providing the Blu Wireless Technology (BWT) platform with some of the findings the task has as outcomes [3][4][5]. As well, deliverable D4.4 [2] aims at using multiple antennas to attain a reliable and high data rate communication in the expected scenarios, overcoming the mmWave propagation disadvantages. Deliverable D4.8 [6] summarises work in these deliverables. In parallel, Task 4.2.2 aims at the development of the 5G-XHaul mmWave transceiver solution, from the chip and antenna design to the analogue front end (AFE) integration [1].

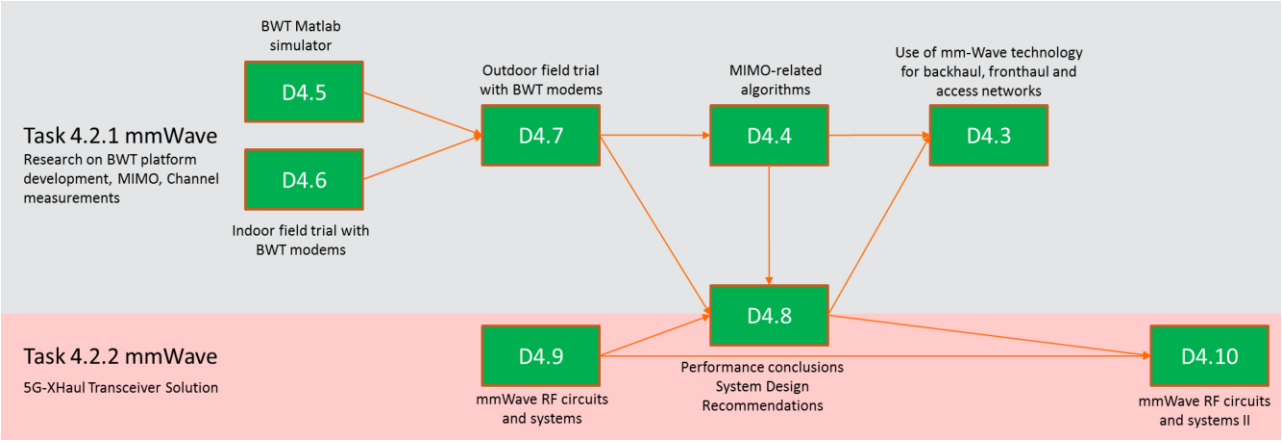

Figure 1-1: Sketch on the technical work belonging to WP4.

This document captures results on mmWave transport that have not been captured in the previous deliverables. In particular, we examine the viability of FH over mmWave links, and the use of meshing to provide resilience and to realise data transfer between nodes that do not possess a direct line-of-sight (LoS). Given the surge of interest in mmWave links for 5G access, the document also looks into methods of joint access and BH.

Organisation of the document

This deliverable is structured in three main sections. Following the introduction section, in Section 2 we evaluate the application of mmWave for fronthauling, using the latest specifications of IEEE 802.11ay to dictate the capabilities of the mmWave links. Section 3 presents the use of mmWave for access and BH links. Meshing of mmWave links is evaluated in Section 4 using a dynamic system simulator. Finally, Section 5 concludes the deliverable.

2 Millimetre Wave for Fronthaul

2.1 Performance of mmWave FH Technologies vs. FH Requirements

In WP2 [11], [12], [13], 5G-XHaul derived requirements for future transport networks. This section compares these requirements against the performance of current and future mmWave technology performance to derive the use cases where mmWave technology can be applied to fronthauling.

State of the Art mmWave Technology

Current mm-Wave products can be separated into those using proprietary technology and those that follow open standards, the most popular being the 60 GHz WiGig standard IEEE 802.11ad [1][8], and its planned successor, 802.11ay [9]. An analysis of available proprietary solutions was composed by the EU-project iJOIN in [10]. These solutions are mainly tailored for the current CPRI standard, i.e. 4G technology. We hence focus on the two mentioned IEEE standards to evaluate their suitability for 5G FH.

Throughput Comparison

Table 2-1 shows the maximum performance of both standards for several configurations. The theoretic maximum PHY-layer rates can be easily derived from parameters such as symbol duration, modulation and coding scheme (MCS), and channel bandwidth. However, in order to compare the performance against the requirements of WP2, the MAC throughput is a more reasonable performance measure, as FH data will be carried as payload. Using the BWT dynamic system simulator the achievable rate measured at the top of the MAC layer has been estimated for an IEEE 802.11ad unidirectional link. At long scheduling periods (see discussion in deliverable D3.1 [14]) the overhead from the beacon part of each beacon interval is low, and the MAC & PHY overhead is about 5% (MAC headers, preamble, PHY header, interframe spacing, Block ACK). With smaller scheduling periods the latency falls, the beacon header overhead increases, and the maximum sustainable rate (max load) falls, Figure 2-1.

If we add another 5% for the beacon part, and some margin for retransmissions (and possible transmitter window stalling), a conservative figure to assume would be 15% total reduction in rate over the headline MCS rate. Hence we have used the assumption of 15% overhead to derive the peak MAC layer throughputs in Table 2-1 for all configurations.

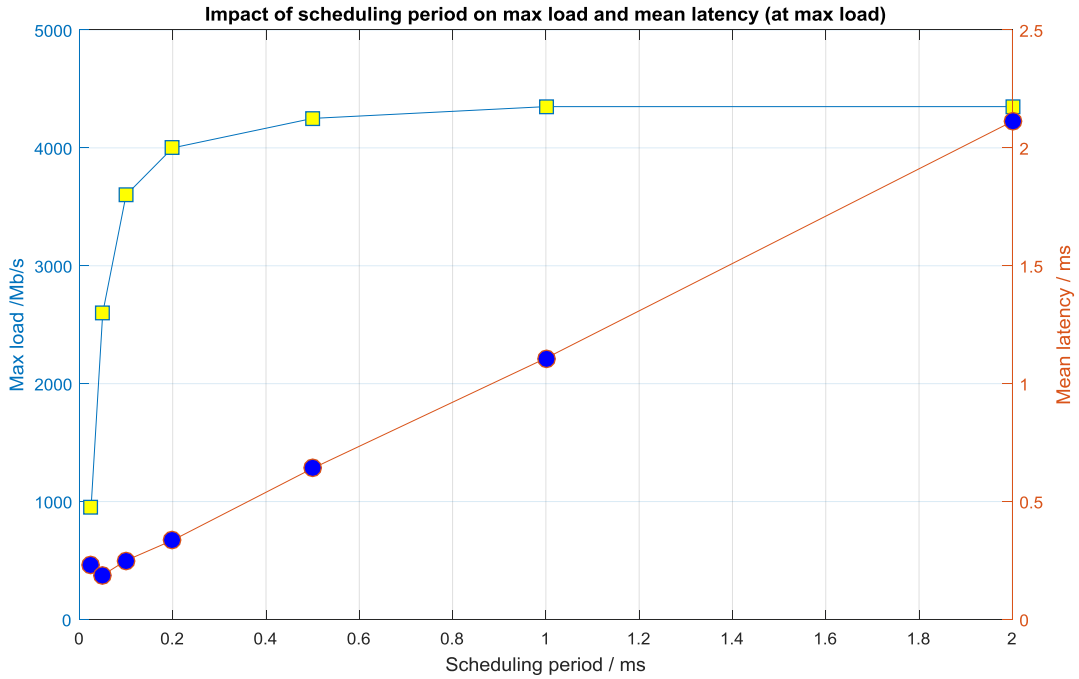

Figure 2-1. Performance trade-offs for an IEEE 802.11ad PBSS with a unidirectional link with rate of 4.62 Gbps (MCS 12).

Table 2-1: Maximum data rates of 60 GHz IEEE 802.11 technologies.

Standard	Configuration	Short name	Max. PHY rate	Max. MAC throughput (15 % overhead)
802.11ad	1 stream, 1 channel	ad 1x1	8.1[1] Gbps	6.8 Gbps
802.11ay	1 stream, 2 channel	ay 1x2	16.2[2] Gbps	13.7 Gbps
	1 stream, 4 channels	ay 1x4	32.3 Gbps	27.5 Gbps
	4 streams, 4 channels	ay 4x4	129.4 Gbps	110.0 Gbps
	8 streams, 4 channels	ay 8x4	258.7 Gbps	219.9 Gbps

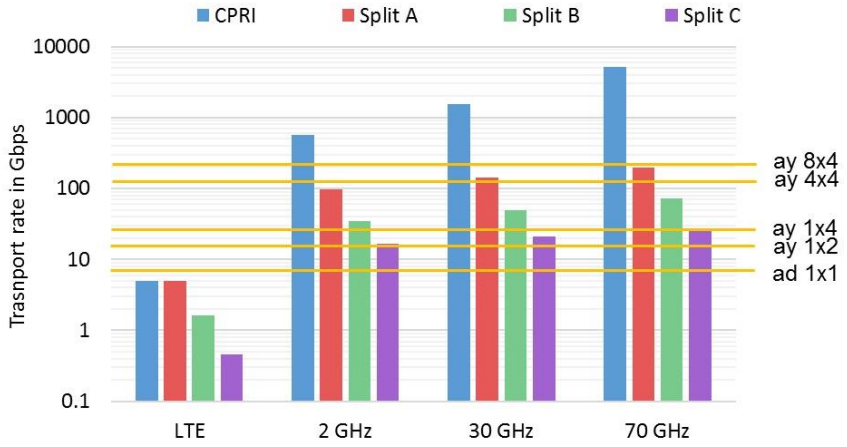

Figure 2-2: mmWave technology throughput performance vs. FH peak data rate requirements.

For IEEE 802.11ay we have listed several configurations, as it supports up to 4 channels and up to 8 streams using MIMO. A channel is 2.16 GHz wide. The minimum channel allocation is 2 for a pair of 802.11ay stations to form a link. While a bundling of channels seems reasonable for FH applications, the use of MIMO heavily depends on the channel characteristics. Especially for rooftop-mounted, fixed point-to-point or point-to-multipoint applications it is still unclear whether high spatial separation can be achieved. Accordingly, the results for the 8x4 configuration of 802.11ay should be viewed with caution. In general, these max. rates can also be only achieved with very good SNRs, hence we assume a best-case scenario here.

Figure 2-2 compares the MAC throughput from Table 2-1 to the peak requirements derived in [11] and [15] for different functional splits and different air interfaces. As can be seen the 802.11ad 1x1 configuration can achieve the required data rates for 4G FH, even for high-demanding splits like split A and traditional CPRI. However, they are unsuitable for the exemplary 5G configurations we derived in WP2.

Taking the reasonable 1x4 (1 stream, 4 channels) configuration of 802.11ay, it is already possible to approximately fulfil the requirements for Split C, as this split is already close to the traditional BH split. Finally, the 8x4 (8 streams. 4 channels) configuration can fulfil all requirements for all splits and air interface, except for the CPRI split. Recalling, that the difference between the CPRI split and split A is that split A avoids the scaling of FH data rate with the number of antennas for massive MIMO, this again points to the necessity to implement new functional splits as discussed in deliverable D2.1 [11].

[1] This is for single carrier mode MCS 12.6 (64QAM code rate 7/8).

[2] This (and other 802.11ay options) assume single carrier mode, 64QAM code rate 7/8, normal GI.

Next, we also compare the 802.11 throughput performance to the aggregate FH data rates derived from real-life measurements in [15], to evaluate the suitability of mmWave technology not only for the last mile, but also for aggregation of several FH links. The comparison is illustrated in Figure 2-3. It can be seen that for 4G LTE, the different 802.11 technologies could be used to aggregate the traffic of between 40 (Split A) and more than 1000 (Split C) cells. However, only the 8x4 and 4x4 configuration can deliver the performance required to aggregate 5G cells, ranging between 1-2 cells for split A and 20-100 cells for split C.

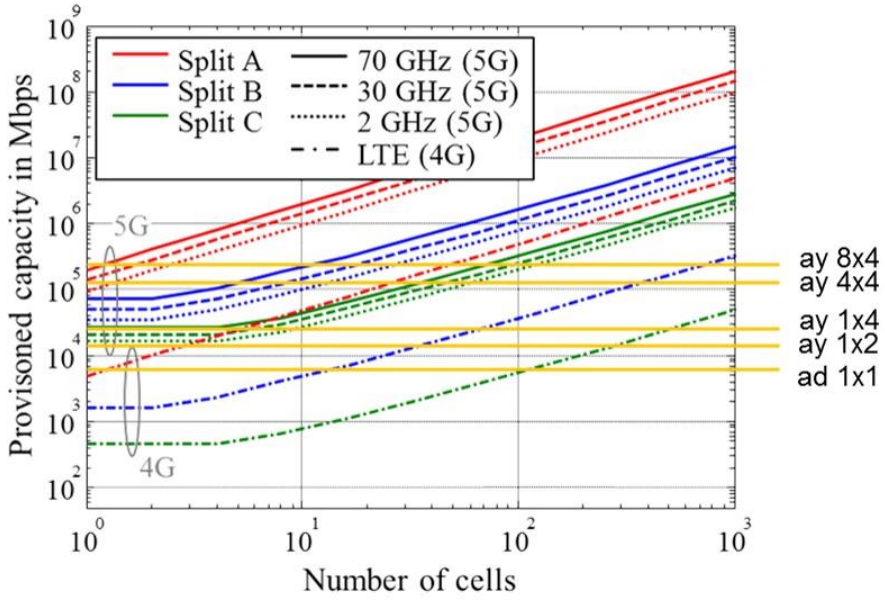

Figure 2-3: mmWave technology throughput performance vs. FH aggregate data rate requirements.

Latency Comparison

As discussed in deliverable D2.1 [11], future FH interfaces also need to fulfil certain latency constraints. However, these constraints are not as clearly derived as the data rate requirements. For CPRI, it is well known that the limitation lies in the HARQ budget of LTE, which is 3 ms (after subtracting the DL receiver processing time, compare [18]). Further subtracting the BB processing time, this results in approximately 250 µs of FH latency budget. Both values are indicated in Figure 2-4 as black lines. However, this could change for 5G networks, depending on the parametrization of PHY and HARQ. Hence, we derived in [15] more fundamental latency limits based on channel coherence time. The basic assumption here is that several adaptive methods (channel estimation, precoding, etc.) are based on channel knowledge and hence, should be performed within the channel coherence time. Figure 2-4 illustrates the channel coherence time, again for the different air interfaces and for different UE speeds.

The achievable latency of mmWave products was evaluated by 5G-XHaul and is available for commercial proprietary solutions. It ranges between 20 µs [7] and around 200 µs [10], [12], for a single hop, which is also illustrated in Figure 2-4.

As can be seen from Figure 2-4, 802.11 latencies are below the requirements based on channel coherence time, except for the mmWave access air interfaces at very high speed. We hence conclude that in principal mmWave technology (with a single hop) is suitable for most FH use cases. However, these results need to be viewed with care, as both the actual 802.11 performance as well as the actual requirements of 5G air interfaces depend on several factors mentioned earlier (HARQ implementation in 5G; contention in mmWave MAC).

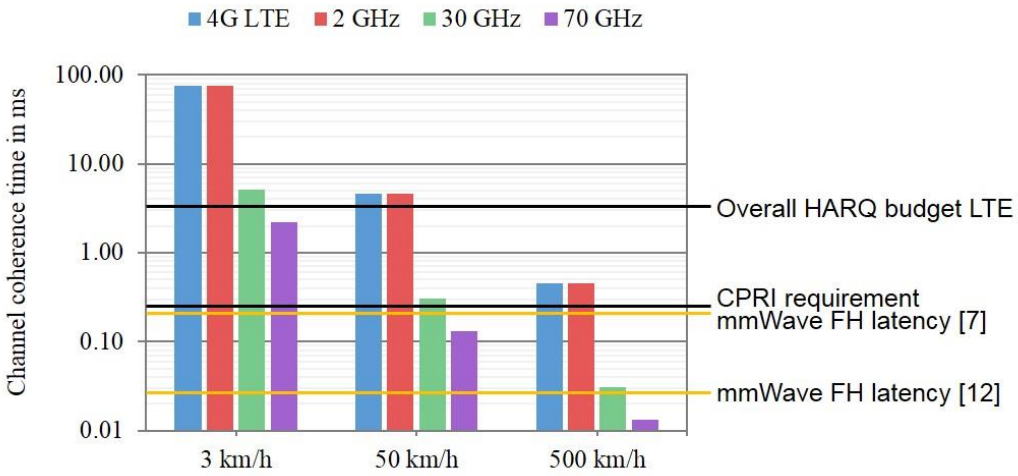

Figure 2-4: mmWave technology latency vs. FH requirements.

Jitter and synchronization via mmWave

The provision of frequency and phase synchronisation over mmWave links was discussed in detail in deliverable D4.13 [20]. In principle, SyncE can provide high accuracy syntonisation, whilst IEEE 1588v2 offers good phase accuracy of the clock. Jitter on the wireless link (or links if there are multiple hops) can be compensated for by the transparent clock mechanism. In terms of jitter in the delivery of the FH payload itself, jitter is likely to be dominated by retransmission events on the mmWave air interface and by the time division duplex (TDD) nature of the link.

This has been studied by the BWT system simulator, and the results are shown in Figure 2-5. Here the delay is measured for traffic passing through a switch over an IEEE 802.11ad link (at MCS12) and through a second switch. The beacon interval [14] is shared between the link from the PBSS Control Point (PCP) to the non-PCP STA, and the reverse link. Since the link *from* the PCP is scheduled first this shows lower latency. With no errors, the delay spread is approximately 125 µs, but this more than doubles with a 1% packet error rate. The time alignment requirement for CPRI is 65 ns, which is required for TX MIMO (to align antenna ports in time). As the 125 µs here is too large, the question is whether the delay could be accurately estimated and the samples aligned with a buffer to reduce the spread. The buffer then just adds to overall latency. Since CPRI is constant rate it would just have to output the frames at exactly that rate. However, such a buffer would need to compensate ALL delay variation, which according to the figure would induce a delay of >1 ms, which is more than the CPRI requirement of ~ 200 µs. For the other splits the requirements would be relaxed as the time alignment would be performed at the remote radio head (RRH) anyway.

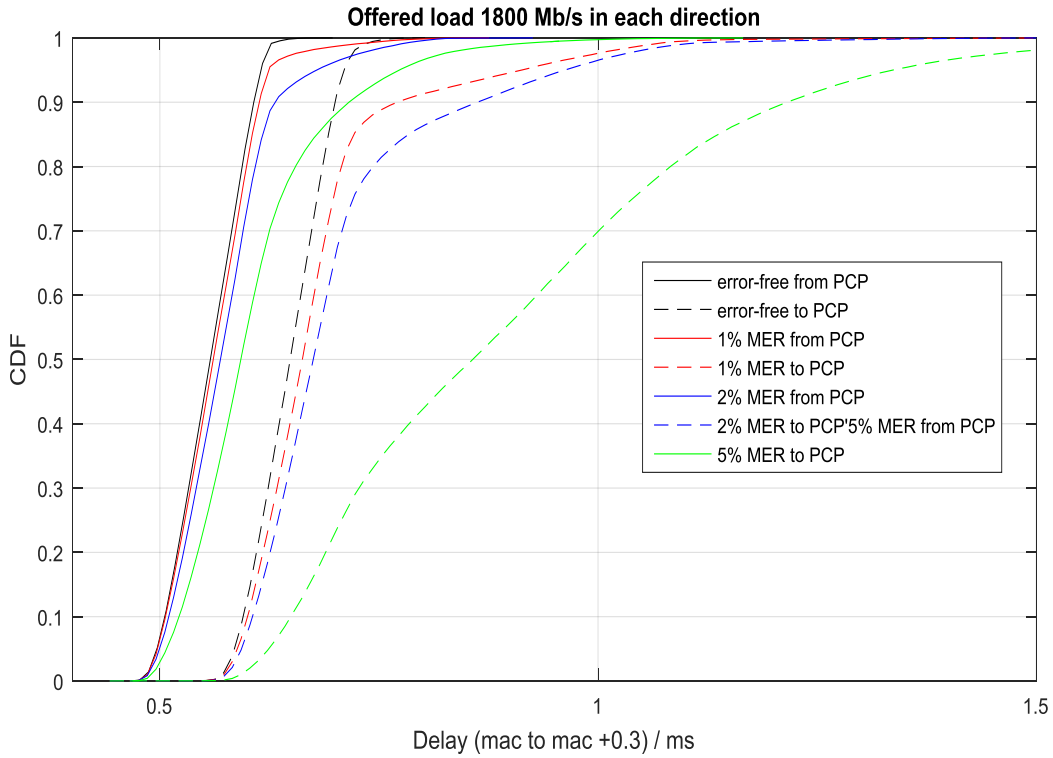

Figure 2-5. Delay between MACs plus a switching time of 0.3 ms for a bidirectional IEEE 802.11ad link loaded with 1800 Mbps of traffic in each direction

3 Joint Design of Access and Fronthaul/Backhaul

3.1 Joint Design of Access and Fronthaul

Although specialized mmWave products are already in use for last-mile FH, they so far have not seen large scale deployment. In order to deliver the benefits of a wireless FH solution to a wider range of use cases, new approaches to mmWave access and FH have to be derived. The concluded EU-project iJOIN pioneered the approach of a joint design of radio access and FH [10]. Such a joint design considered both wireless segments to derive more coordinated approaches in order to improve network performance. These approaches ranged from the PHY- over the MAC- to the Network layer, covering such aspects as joint detection and decoding, joint scheduling and cell selection, or optimized routing.

One general challenge in mmWave communications is the strong attenuation of the radio waves by precipitation [21]. Accordingly, it is important to design mmWave FH links for, e.g. rainy scenarios. Conventionally, this can be done by either adaptive modulation and coding (AMC), or by allocating a corresponding margin in the link budget. As both methods have disadvantages (variable throughput in case of AMC, lower range in case of a margin), an alternative solution was derived in 5G-XHaul, which is also reported in [16], [17]. This alternative method is based on a joint radio access and FH receiver, which is summarized in the following text. The full details can be found in the previously given references.

The joint receiver is based on the principle that the unreliability of FH links due to precipitation is not avoided by AMC or a link budget margin, but taken into account by the radio access receiver. In FH scenarios where one of the lower functional splits (A, B) is implemented, the user data is encoded at the UE for the RAN link and only decoded in the baseband unit (BBU). Therefore, it is protected against errors while on the FH link. We can hence cope with FH unreliability, provided that it is considered in the RAN receiver. For this, the RAN and FH links are not seen as separate, but as one joint link. This concept is illustrated in Figure 3-1.

The underlying concept of the joint receiver is a joint minimum mean square error (MMSE) estimation of the I/Q-symbols transmitted over the FH link. The principal can be illustrated by the following formula:

$$\hat{x} = \frac{\int x' \sum_x p(x)p(x'|x) \prod_b p(q'_b|q)\,\mathrm{d}x'}{\int \sum_x p(x)p(x'|x) \prod_b p(q'_b|q)\,\mathrm{d}x'}, \tag{3.1}$$

where x is the symbol transmitted from the UE, x' is the symbol received at the RU after RAN transmission, q is the digitized received symbol before the FH and q'_b is the b-th bit of the received digitised symbol after the FH. $p(x'|x)$ denotes the symbol transition probability of the RAN and $p(q'_b|q)$ of the FH channel. Finally, $\hat{x}$ is the jointly estimated symbol at the central unit (CU), which is used to calculate the soft information that serves as input to the RAN decoder. Basically, the reliability information of the FH channel, $p(x'|x)$, is taken into account when calculating the radio access channel's soft information.

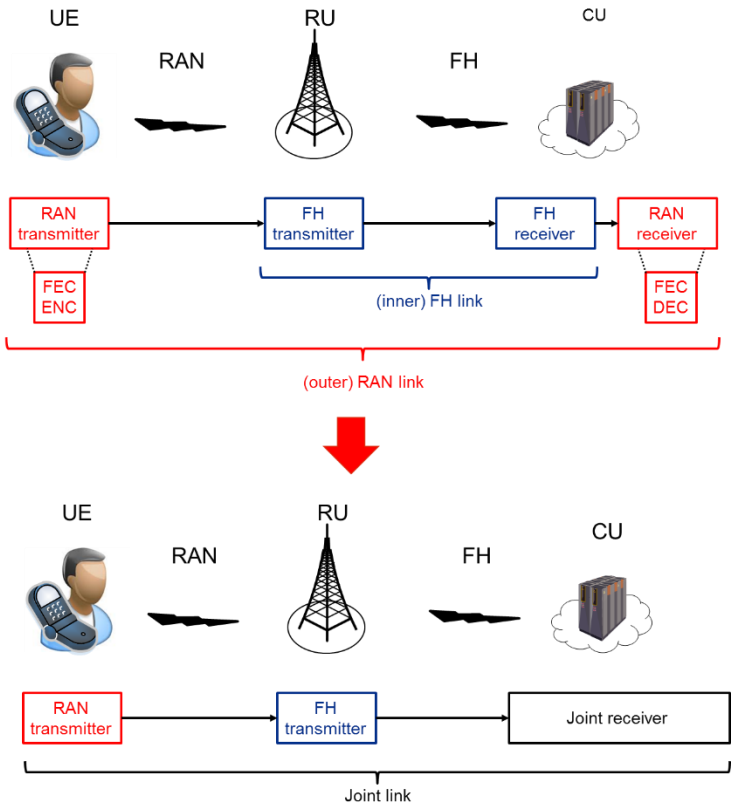

Figure 3-1: Principle of joint radio access and FH receiver.

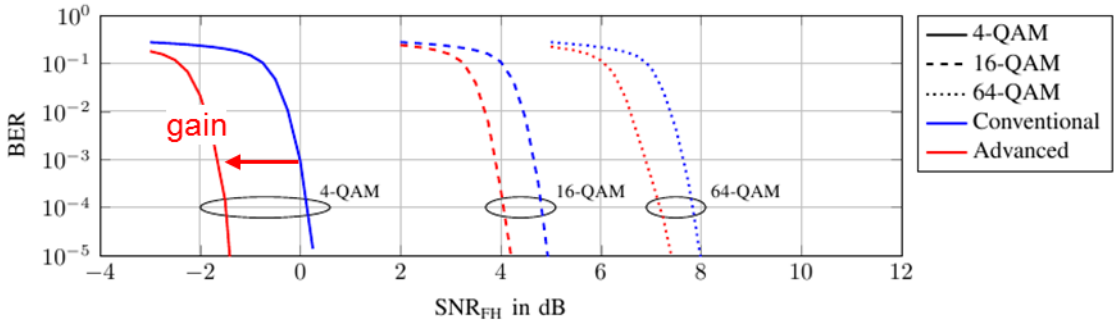

Figure 3-2: Single-link BER performance of joint radio access and FH receiver compared to traditional receivers.

This joint receiver now yields good end-to-end (from UE to CU) bit error rates (BERs), even when the FH is unreliable. The performance gain over conventional, separate receivers is illustrated in Figure 3-2. As can be seen, a gain of up to 2 dB in SNR can be achieved.

Adopting this to a larger scenario as described in [17], Figure 3-3 shows an end-to-end throughput improvement of up to 81%, compared to conventional receivers, and showing equal performance to encoded FH (as would be the case for e.g. 802.11-based FH), which however requires a separate FH en- and decoder. As can be also seen, the joint receiver offers no benefit in scenarios without rain. As it was designed to cope with unreliable FH links, it does not yield gains in scenarios where the FH is already very reliable, which is the assumption for the “no rain” scenario.

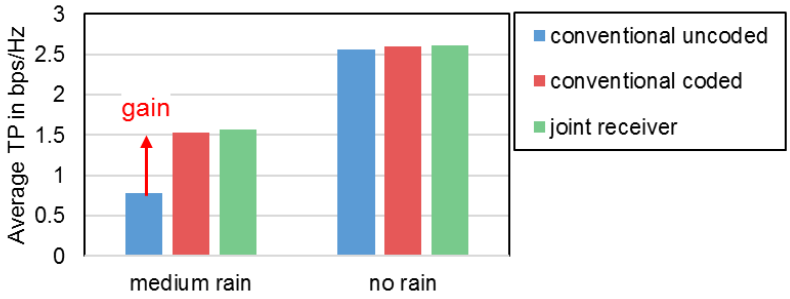

Figure 3-3: Throughput comparison of joint and conventional receiver for different scenarios [17].

The joint receiver is not limited do data channels, but can be also applied to, e.g. synchronization channels (the random access channel, RACH) or for reference symbols required for channel estimation. However, the joint receiver also faces several disadvantages. One is the higher complexity, which needs to be weighed against the complexity reduction by avoiding separate FH coding, the other is that it requires a co-location of FH and RAN receiver at the same location, and preferably even on the same hardware. Finally, it is only applicable to the uplink, and new concepts will need to be applied to adapt the concept of unreliable FH to the DL as well.

3.2 Wireless Self-backhauling

Small cells are to play a key role to cope with the increasing traffic demands in mobile network. These small cells connect to the core network via wired or wireless BH links. The dense deployment of small cells and variety of services offered by the RAN having diverse requirements on throughput, latency and reliability, possess new challenges on BH links. One way to address these challenges is *self-backhauling*, i.e., the access and BH share the same wireless channel.

3GPP stage 1 in its Release 16 [23] outlines the requirements for the self-backhauling in 5G networks. Among these requirements are the flexible partitioning of resources, autonomous configuration, multi-hop wireless connectivity, topology adaptation, and redundant connectivity. We explain how these requirements can be fulfilled using an example deployment of the small cells in 5G-network in Figure 3-4.

3.2.1 Redundant Connectivity

This requirement facilitates the adaptability, high throughout and high reliability needs of the 5G enabled devices. Here the next generation eNB has multiple BH links (either wireless or wired) to enable a multi-link connectivity and adaptability. This multi-connectivity can be used to either increase capacity or reliability. On the other hand, multiple BH links allow to select the route to the core network with minimum delay. Hence providing a flexible and adaptive network.

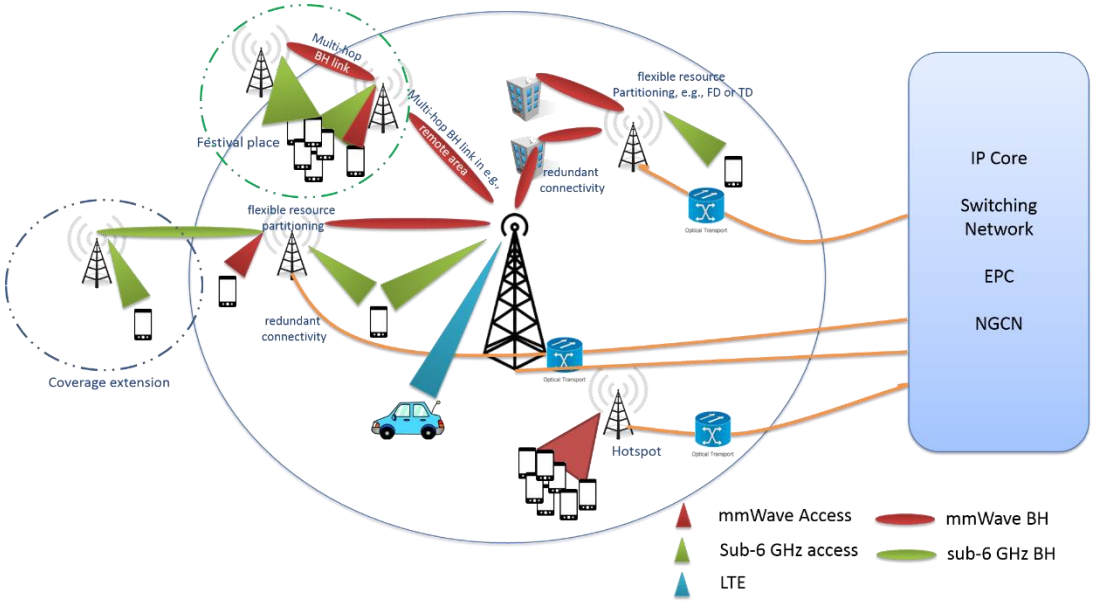

Figure 3-4 Example scenario with self-backhauling.

3.2.2 Autonomous Configuration and Topology Adaptation

Autonomous configuration and topology adaptation are two crucial requirements for the deployment of small cells in the 5G network. Since small cells are needed to serve hotspots in the area, which are time dependent, the topology adaption is a key feature required for self-backhauling. Consider a public square where user density depends on various factors, e.g. day and time of the week, weather, etc. Hence these hotspots can be switched-off during the off-peak times, which requires the network topology to be adapted. Similarly, when these hotspots need to be active again, they must be capable of configuring themselves.

3.2.3 Multi-hop BH links

Multi-hop links are crucial to cover the last mile in the deployment of network when fibre deployment is cumbersome or not cost-effective. This allows operators to flexibly extend the coverage of the network and adapt the network to the traffic needs. However, one should take into account the delay and protocol overhead needed for multi-hop BH links. An evaluation of a multi-hop BH network is presented in chapter 4.

3.2.4 Flexible Resource Partitioning

MmWave plays an important role to provide 1000x increase in capacity for BH. However, the mmWave is also needed in access to meet the high capacity requirement of 5G enabled devices. Hence, flexible resource partitioning between access and BH is very important. Here we refer ‘space’, ‘frequency’ and ‘time’ as the fundamental resources of the network. MmWave provides a unique opportunity because of availability of large bandwidth and beamforming capability. The resources can be shared between BH and access partially or fully as depicted in Figure 3-5. In case of partial resource sharing, the frequency division or time division multiplexing can be utilized, whereas due to beamforming the full bandwidth can be simultaneously utilized both for access and BH.

Regarding resource partitioning of Sub-6 GHz, this plays an important role in connecting small cells with NLoS connectivity in urban areas (street level). Here resources of access network can be shared partially between BH and access.

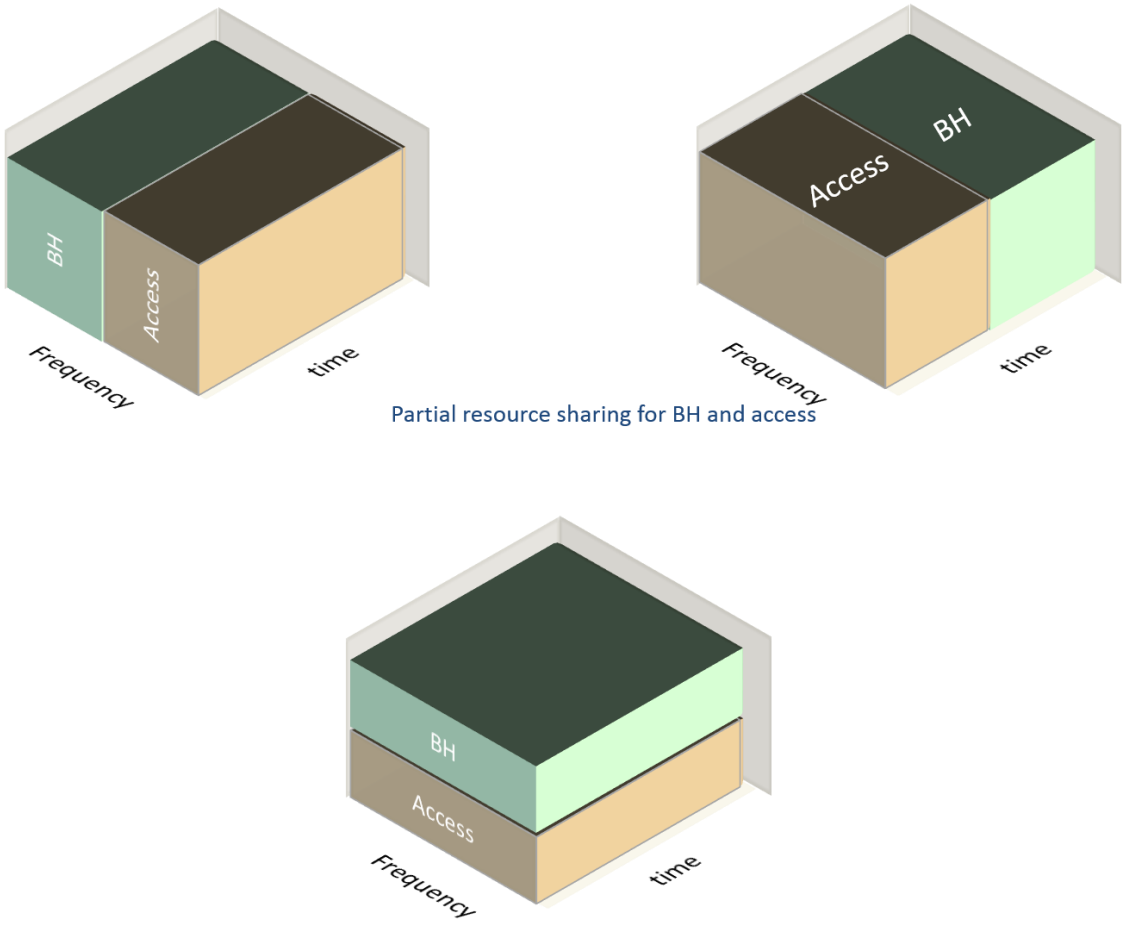

Figure 3-5: Possibilities for resource sharing between access and BH.

4 Millimetre Wave Meshed Backhaul

In some mmWave wireless BH deployments, the small cell or RRH cannot be backhauled/fronthauled by a single wireless link. Typical reasons are that the span to the POP (point of presence, aka gateway) is too long or blocked by buildings or other obstructions. In these circumstances, a multi-hop connection can be established. If there are more than one possible multi-hop paths to the POP then the wireless BH network is described as meshed. This offers resilience in the event of a link failure and provides additional capacity for load balancing and other traffic engineering functionality.

In this section, we model a meshed BH network mapped to a cellular deployment in the *Eixample* district of Barcelona, as previously studied in deliverable D2.4 [22]. The objective is to assess the BH bandwidth per small cell and the latency to the POP. The cellular deployment is shown in Figure 4-1. There are 3 macro sites (nodes 4, 8,17), with fibre backhaul that are POPs, and 16 small cells. The red rectangles represent potential clustering of small cells to POPs. The blocks are 133.3 m x 133.3 m (street centre to street centre), giving an inter-site distance for adjacent small cells of 66.7 m. In the simulations, each node was offset from the ideal grid by a random distance within the range of +- 5 m in x and y directions to reflect the difficulty in the site placement.

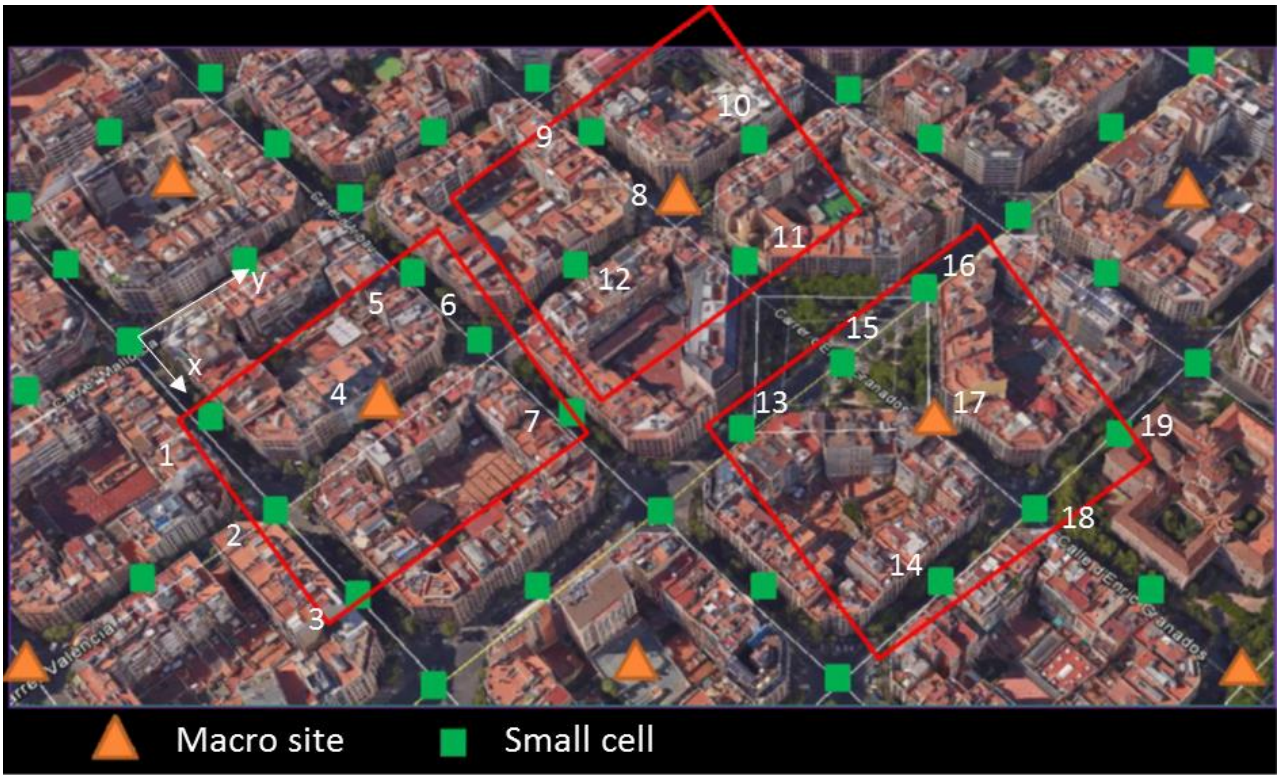

Figure 4-1. Cellular deployment under study.

The BWT dynamic system simulator was used to model the BH network. This assumes that the links are formed using IEEE 802.11ad modems employing phased array patch antennae operating in the V-band (60 GHz). Some simulation assumptions are captured in Table 4-1.

The simulator follows a sequence of steps:

1. Calculate the path gain matrix between nodes.
2. Design the PBSSs and assign channels.
3. Perform route calculation and evaluate the network performance (static simulation).
4. Perform dynamic system simulation.

Table 4-1. Simulator features.

Feature name	Feature support	Notes
Mesh topology	Supports generic topologies of mesh nodes, where each mesh node comprises a switching element and four IEEE 802.11ad STAs. The definition of the PBSSs is part of the topology. Support PBSS with more than two stations (STAs).	
Routing calculator	Route calculation using Dijkstra method	
Radio Model	Thermal noise, worst-case interference, worst-case SINR, worst-case link throughput (and MCS) calculation	Path gains (including antenna gain) for links between STAs of a PBSS that beamform to each other, and path gains of interfering links/beams, are calculated using free-space model (Friis Equation). STAs that do not have line of sight of each other have zero path gain.
	Antenna gain=21 dBi, transmit power 17dBm	
	Rain and oxygen attenuation (combined) 25dB/km	
	Rate adaptation between MCS 1 and MCS12	Single carrier mode of IEEE 802.11ad (OFDM mode is now discontinued in the specification)
Traffic generation models	Constant bit-rate, constant bit-rate with jitter	The constant bit-rate with jitter traffic was used with variable packet size (IMIX). The rates were set equal for all nodes, and at values which the most heavily loaded links could support, without searching exhaustively for the maximum sustainable load.
MAC model	Scheduling of transmissions between STAs within each PBSS using Service Period Access	No support for spatial re-use (two STAs in same PBSS transmitting at same time) or relay
	Beacon header interval	
	Aggregation as specified in IEEE 802.11ad	
	Error probability per MAC protocol data unit (MPDU)	Configurable, set to 1%
	Block ACK	IEEE 802.11-2016 Block ACK scheme
	Simulated time	500 ms
Delay modelling	Switching delay, delay MAC to switch, delay within the MAC (ingress queue, QoS queueing, retransmission queue, air interface transmission delay, reordering queue delay at receiver)	Switch delay=0.15 ms, delay MAC to switch=0.07 ms, scheduling advance=0.1 ms, max pkt rate =2 x10^6/s
Output KPIs	Throughput, latency per packet, queue depth, buffer memory fill (Tx (transmit) or Rx (receive)), inter-link interference matrix, link SINR	

4.1 Single channel (reuse 1) performance assessment

The interference in the network is maximised in the case of a single 2 GHz channel. This is potentially very problematic in grid deployments, like the one chosen, when multiple nodes are placed on a line with no intervening obstructions. A receiving antenna may be aligned directly towards the antenna of an interfering transmitter. This is exacerbated when the nodes are closely spaced, such that the path gain reduction for an overshooting transmission is small. The performance can then be interference-limited. An example of overshoot is shown in Figure 4-2. The transmission from link 1 (Tx1-Rx1) overshoots to add interference at Rx2 which is attempting to receive data from Tx2 (link 2).

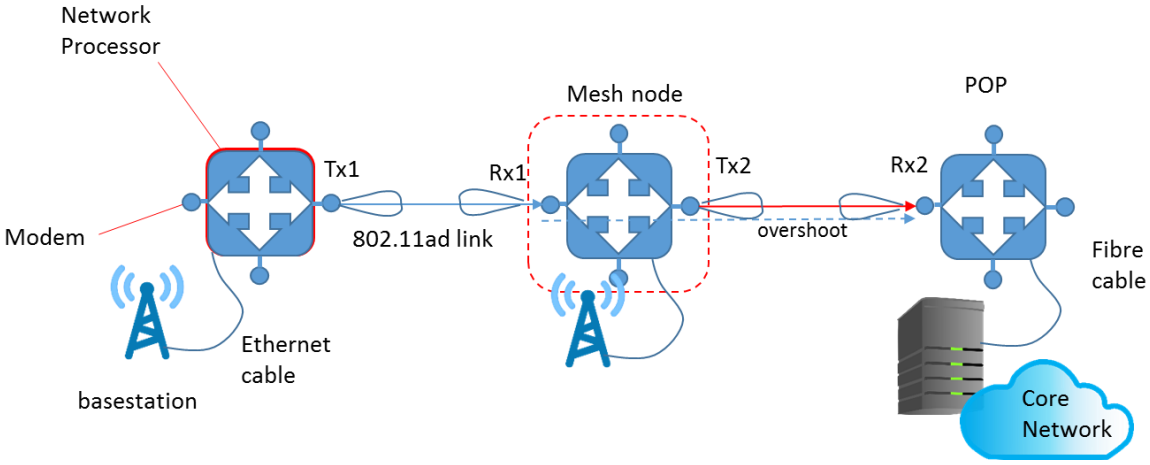

Figure 4-2. Interference from overshoot of radiation when nodes are co-linear.

The PBSSs designed by the simulator are shown in Figure 4-3. Most PBSSs have only two STA, with the PCP being marked by a circle. However, in the upper right there are some 3-member PBSSs. When the routing algorithm is run some of the links are not used, and we can see that each gateway serves a cluster of nodes, Figure 4-4.

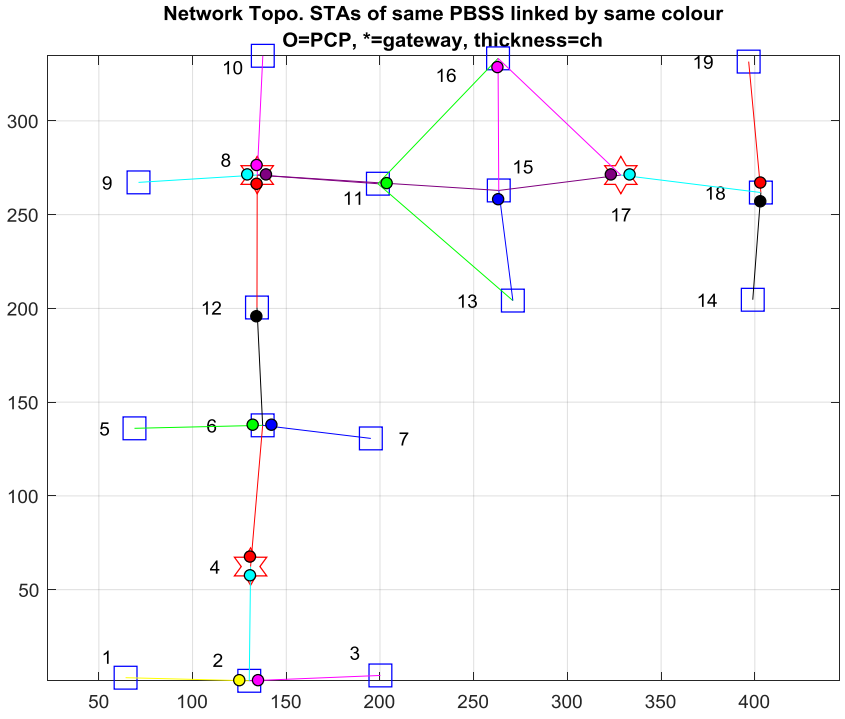

Figure 4-3. Network design of IEEE 802.11ad modems assigned to PBSSs (reuse 1, 3 POPs).

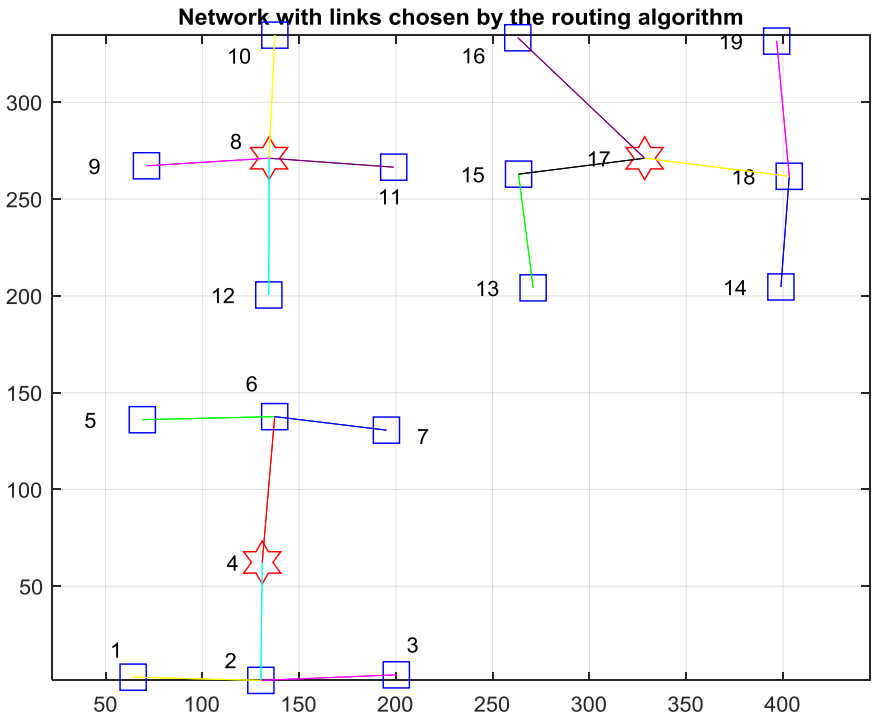

Figure 4-4. Network link chosen by the routing algorithm (reuse 1, 3 POPs).

The impact of the interference is evident in Figure 4-5. Without interference, all links would operate at MCS12 (4.6 Gbps) since the SNR values are very high (the assumed SINR for MCS12 is 13. dB). With interference, four of the 32 routable links drop to MCS7 (1.92 Gbps). In cases where the interference is high, there is typically a single strong interferer, see Figure 4-5(b).

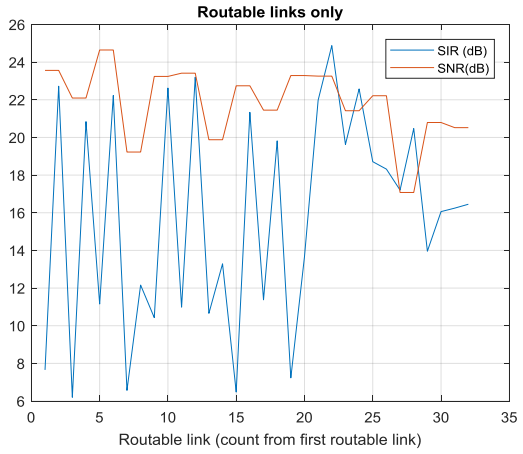

(a)

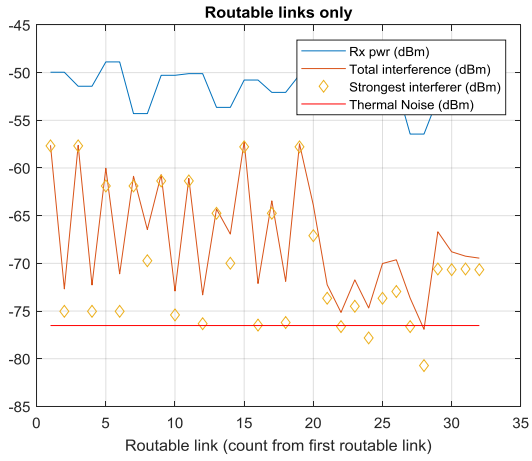

(b)

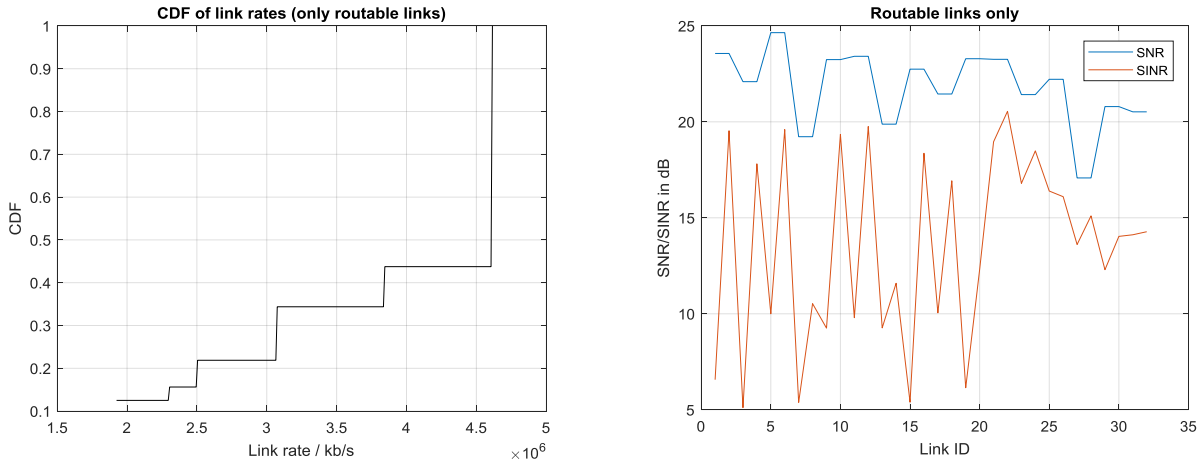

(c) (d)

Figure 4-5. Impact of interference (reuse 1, 3 POPs).

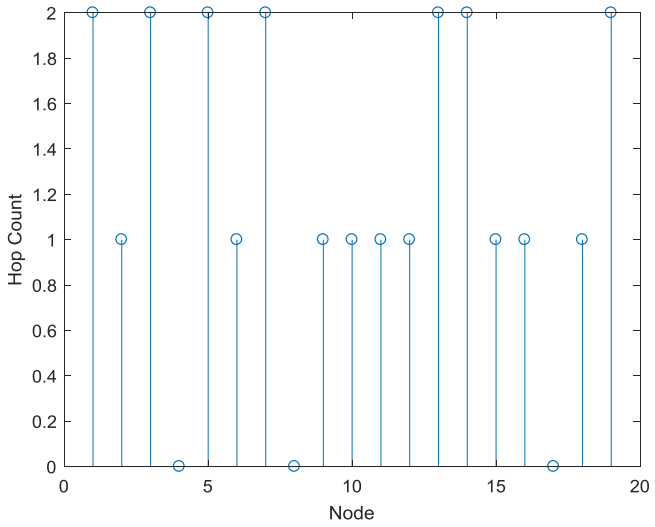

Figure 4-6. Hop count (reuse 1, 3 POPs).

The hop count per node is shown in Figure 4-6. At most there are two hops to a POP/gateway.

If we introduce power control, it should then be possible to reduce interference and thus push up the rates of some of the links. A simple power control algorithm was tested: the Tx power of a MCS12 link is reduced so that the SINR value falls to the minimum value to support MCS12 (13.5 dB). Given that 40% of the candidate links for the routing algorithm (i.e. all the PBSS links) support MCS12 there is scope to raise the performance of other links. This can be seen in Figure 4-7.

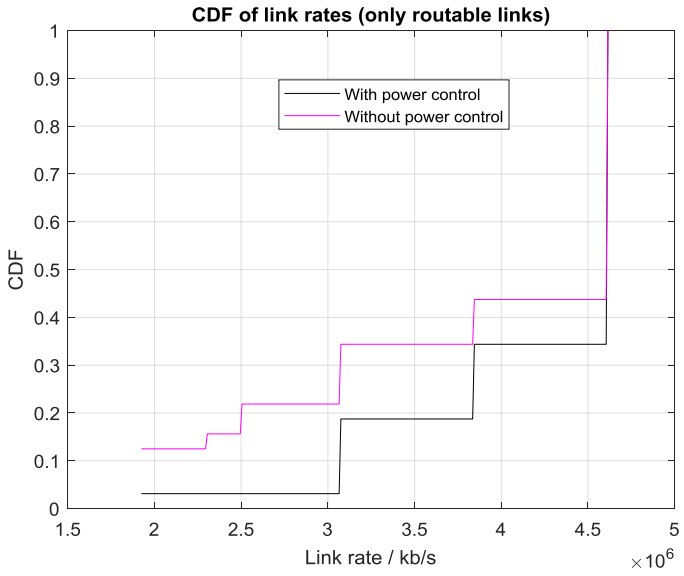

Figure 4-7. Comparison of link rate CDFs with and without power control.

For the dynamic simulation, we assumed that there was no power control because this functionality is dependent on the capabilities of the hardware (baseband and RF). The source traffic rate per node (uplink) was set to 100 Mbps, and the sink rate (downlink) 450 Mbps. This could represent the BH needs of a very high performance LTE small cell (with carrier aggregation, MIMO), or the FH needs of an LTE cell using split C (see Figure 2-3).

The link rates are sufficient to serve the offered rate, even on links to the gateways which carry aggregated traffic. For example, the link between nodes 2 and 4 carries 1.65 Gbps total traffic (associated with nodes 1, 2 & 3).

Throughput and latency metrics are shown in Figure 4-8, Figure 4-9 and Figure 4-10. It is evident that the mean latency is approximately 0.5 ms per hop, for downlink or uplink. Thus, multiple hops will not meet the latency needs of CPRI or split A FH. Even with a single hop, the mean round-trip latency can only be reduced to approximately 100 µs by sacrificing throughput to 800 Mbps for MCS12 [12]. This again indicates the need for new, less delay-sensitive, functional splits to enable the utilization of today`s IEEE 802.11ad mmWave technology for FH.

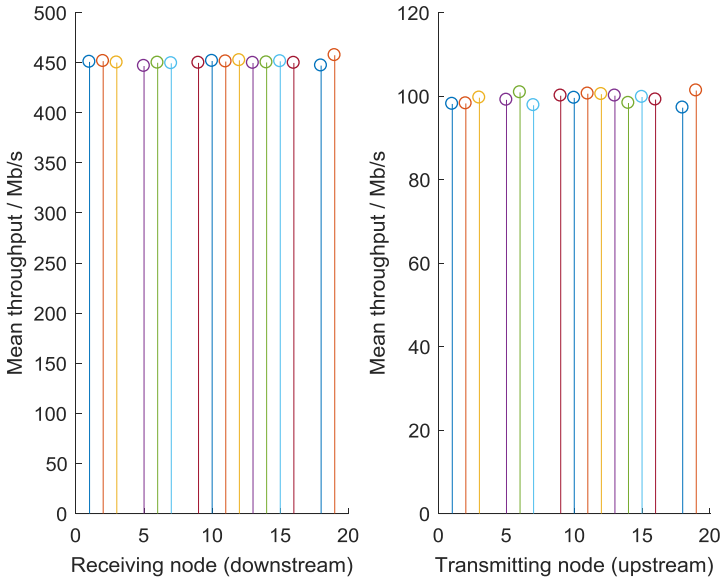

Figure 4-8. Throughput per node (reuse1, 3 POPs).

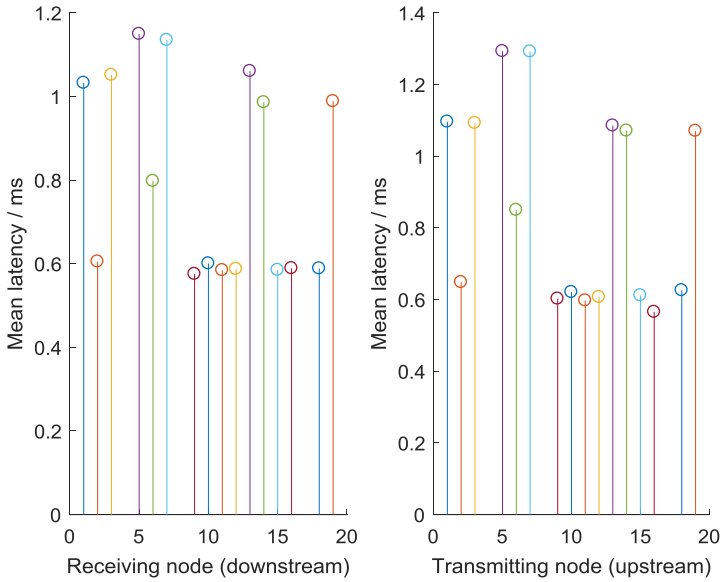

Figure 4-9. Mean latency per node (reuse1, 3 POPs).

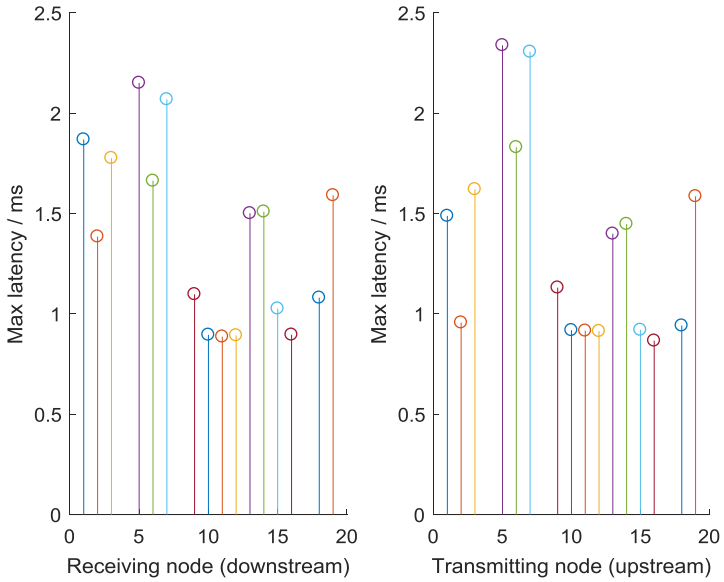

Figure 4-10. Max latency per node (reuse1, 3 POPs).

4.2 Multiple channel (reuse 3) performance assessment

In Europe, three IEEE802.11ad 2 GHz channels are available. Here we add a 3-channel frequency allocation to the network planning to see the performance benefits. Power control is disabled. The channel assignment and PBSS design are shown in Figure 4-11, and Figure 4-12 shows the PCP locations.

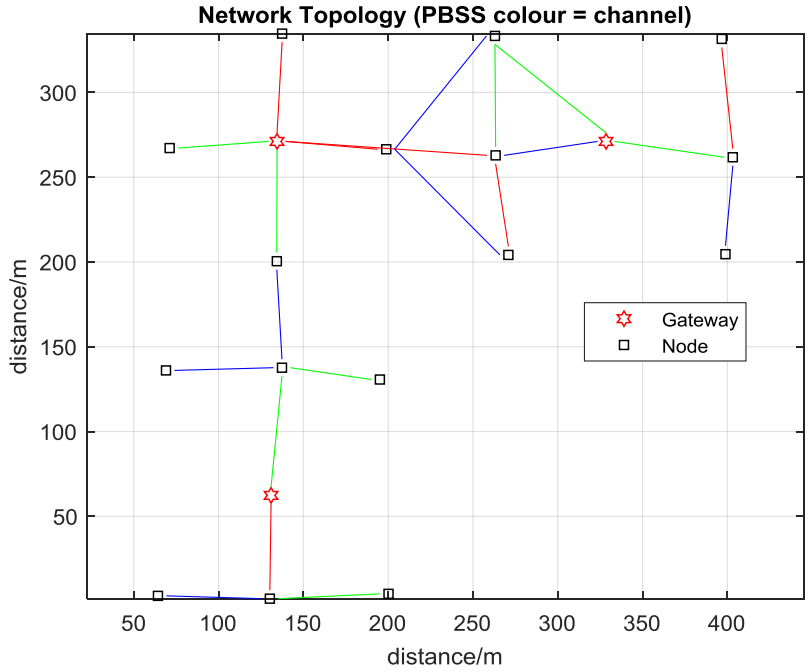

Figure 4-11. Network design of IEEE 802.11ad modems assigned to PBSSs showing colouring /channel assignment (reuse 3, 3 POPs).

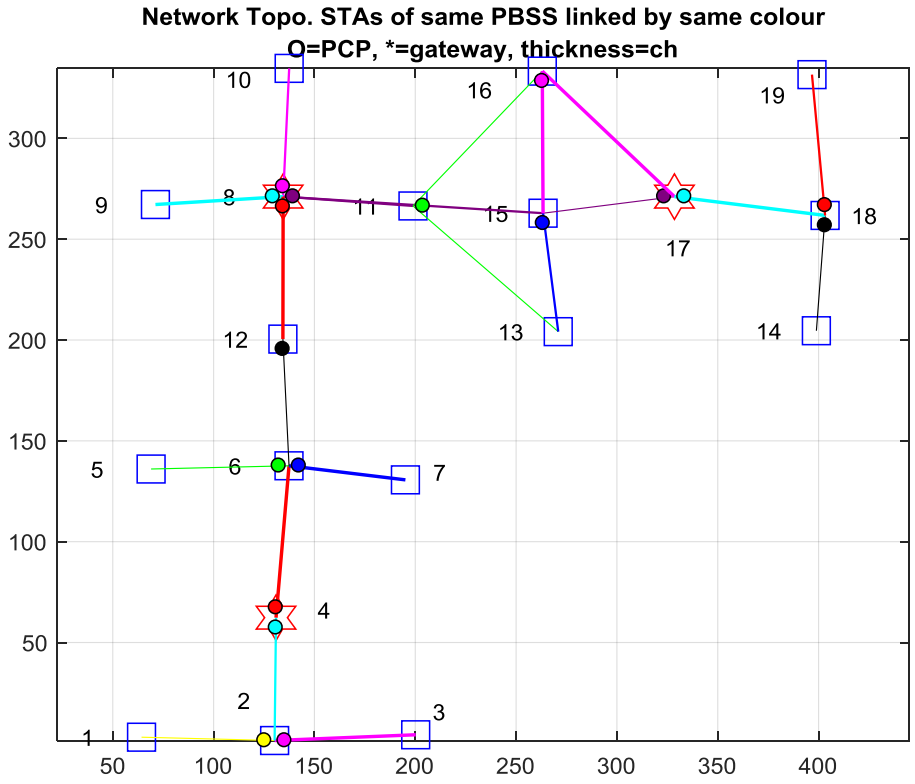

Figure 4-12. Network design of IEEE 802.11ad modems assigned to PBSSs (reuse 3, 3 POPs).

The network links chosen by the routing algorithm are the same as with reuse 1 (see Figure 4-4). Looking at the interference related plots in Figure 4-13, it is clear that the interference is markedly reduced by the channelisation, with many links being thermal noise limited (sub-figure (b)). All routable links now work at MCS12.

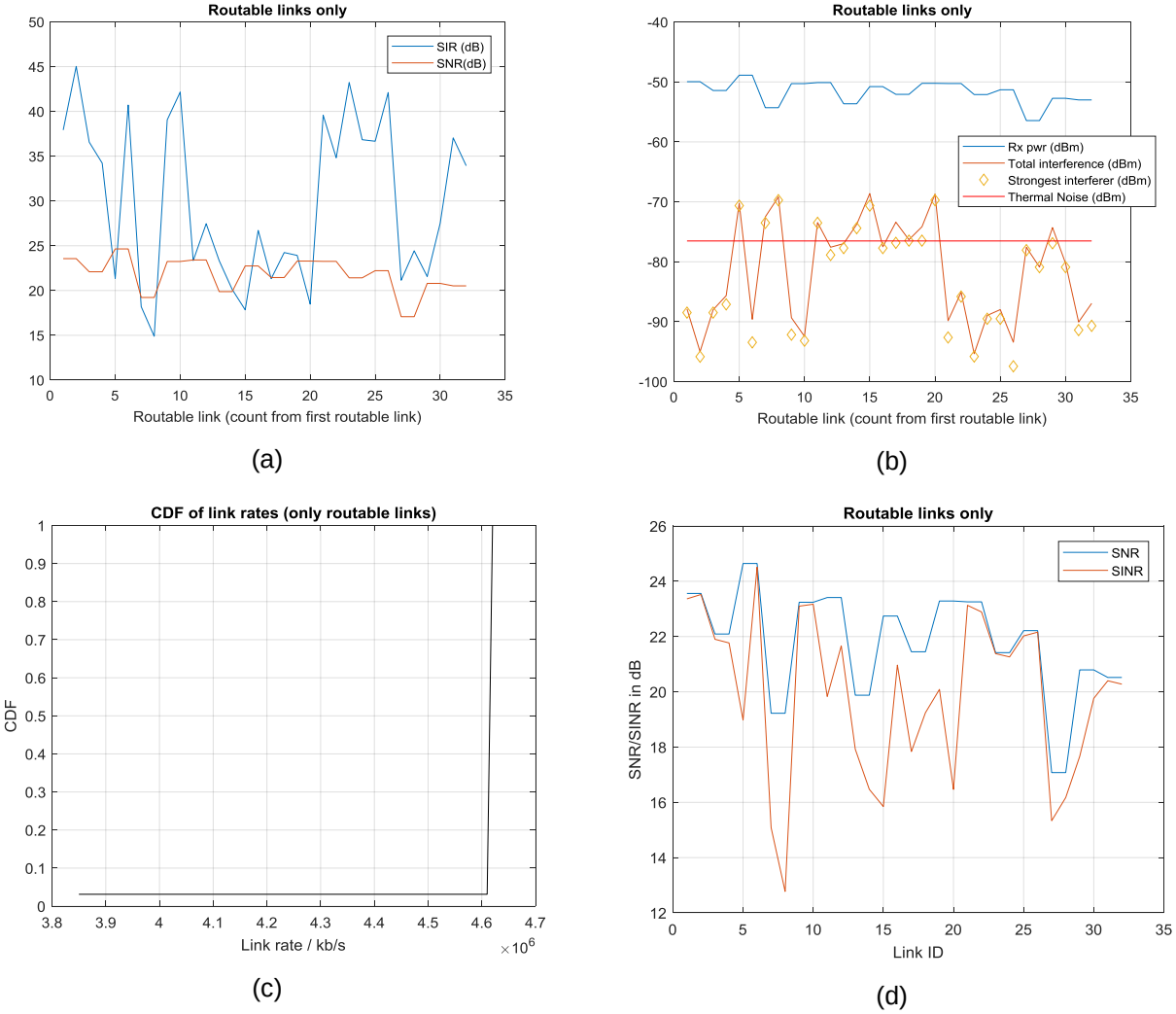

Figure 4-13. Impact of interference (reuse 3, 3 POPs).

The hop count is unchanged from the reuse1 case (see Figure 4-6).

If we use the same offered traffic rates as the reuse 1 scenario (450 Mb/s downlink, 100 Mb/s uplink) there is a small reduction in latency, and the same throughput is maintained.

However, the higher link rates mean that we can increase the traffic rates, to 750 Mbps (DL) and 250 Mbps (UL). Throughput and latency metrics are shown in Figure 4-14, Figure 4-15 and Figure 4-16. It is evident that the mean latency is approximately 0.5 ms per hop, for both downlink and uplink, with the maximum latency being approximately twice the mean value.

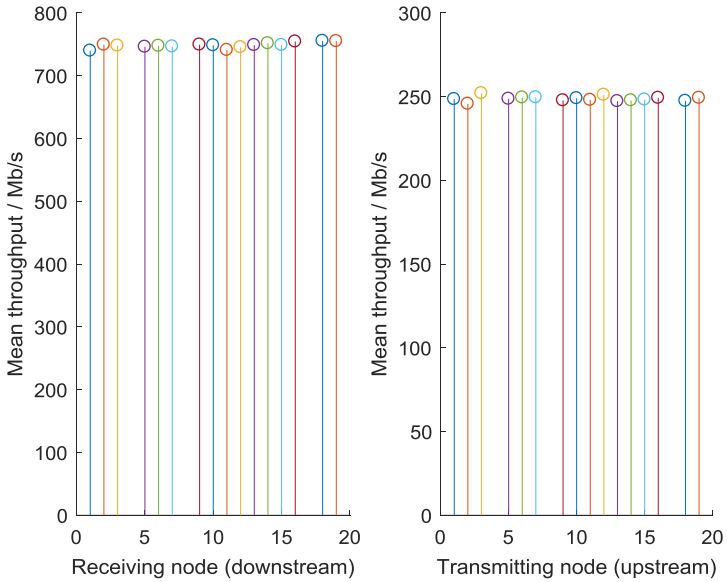

Figure 4-14. Throughput per node (reuse3, 3 POPs).

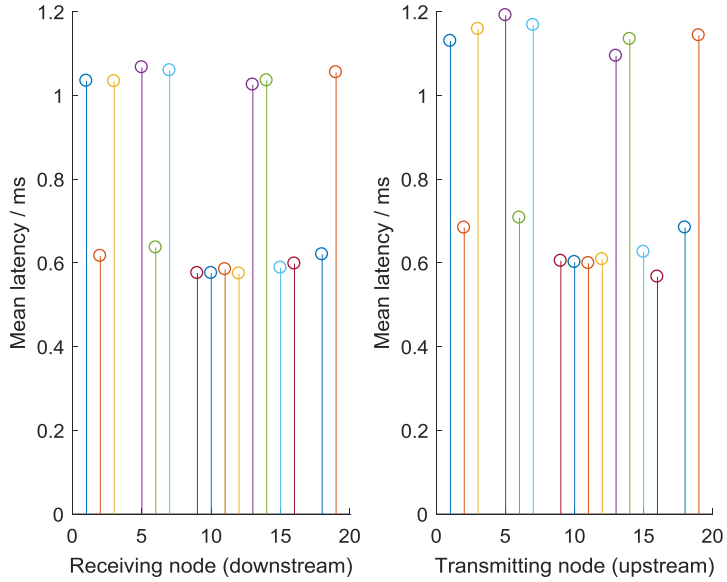

Figure 4-15. Mean latency per node (reuse3, 3 POPs).

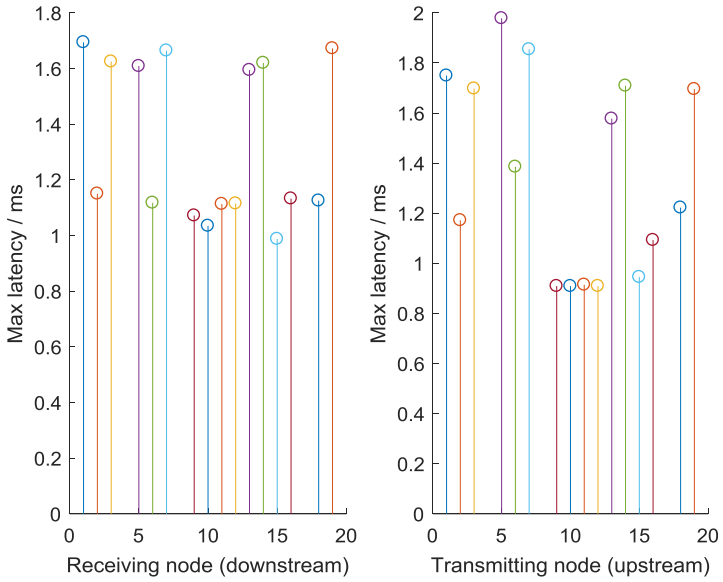

Figure 4-16. Max latency per node (reuse3, 3 POPs).

4.3 Single POP performance assessment

To evaluate the influence of the number of POPs the fibre BH from nodes 4 and 17 were disabled leaving a single POP at node 8. This will increase the hop count, raising the latency, and reduce the BH rates of the nodes because of the aggregation of traffic from the nodes.

The PBSS designs are shown in Figure 4-17 and Figure 4-18. The design algorithm has chosen a number of 3 STA PBSSs. When the routing algorithm is applied the links selected form a tree topology, with the unused links available for failover, Figure 4-19.

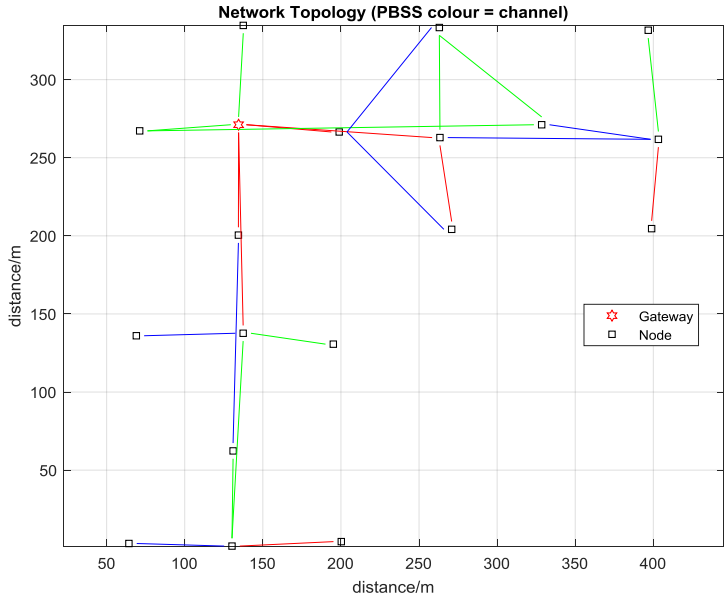

Figure 4-17. Network design of IEEE 802.11ad modems assigned to PBSSs showing colouring /channel assignment (reuse 3, 1 POP).

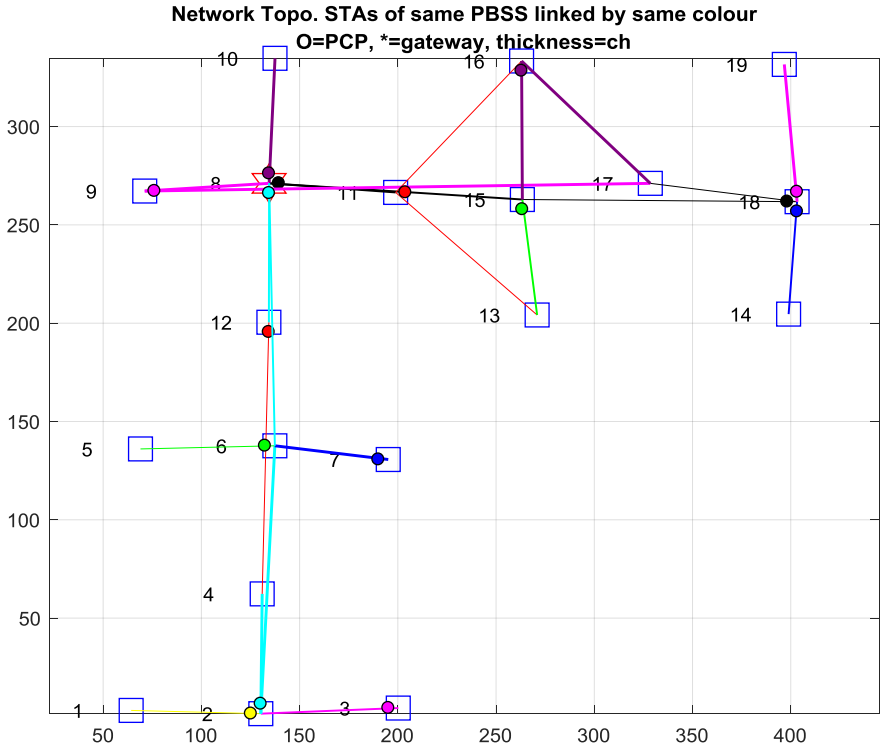

Figure 4-18. Network design of IEEE 802.11ad modems assigned to PBSSs (reuse 3, 1 POP).

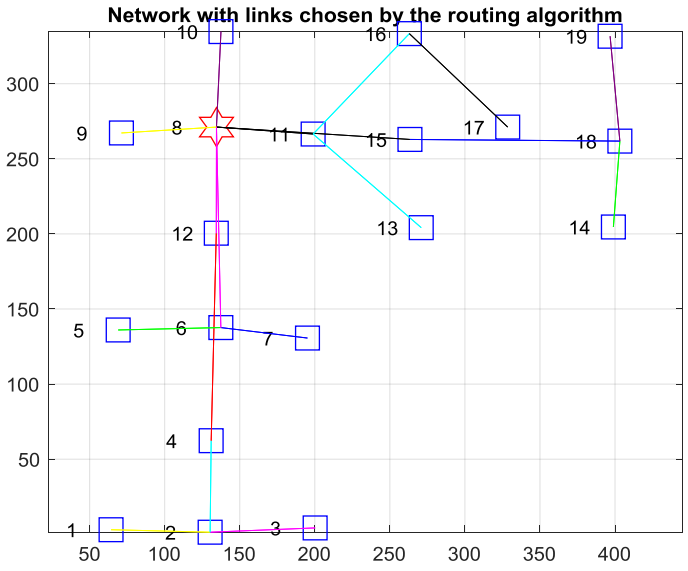

Figure 4-19. Network link chosen by the routing algorithm (reuse 3, 1 POP).

The hop count is increased over the 3 POP networks studied above, with two nodes requiring 4 hops to reach the POP, Figure 4-20.

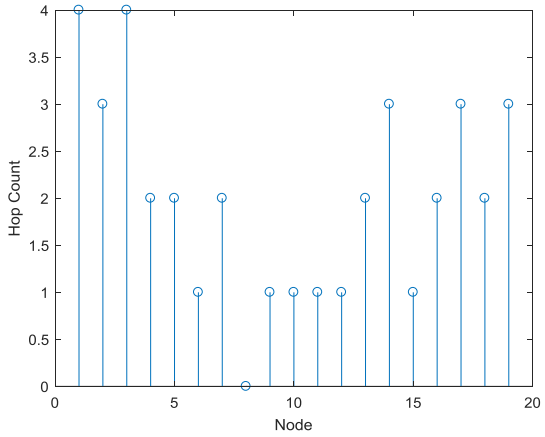

Figure 4-20. Hop count (reuse3 1 POP).

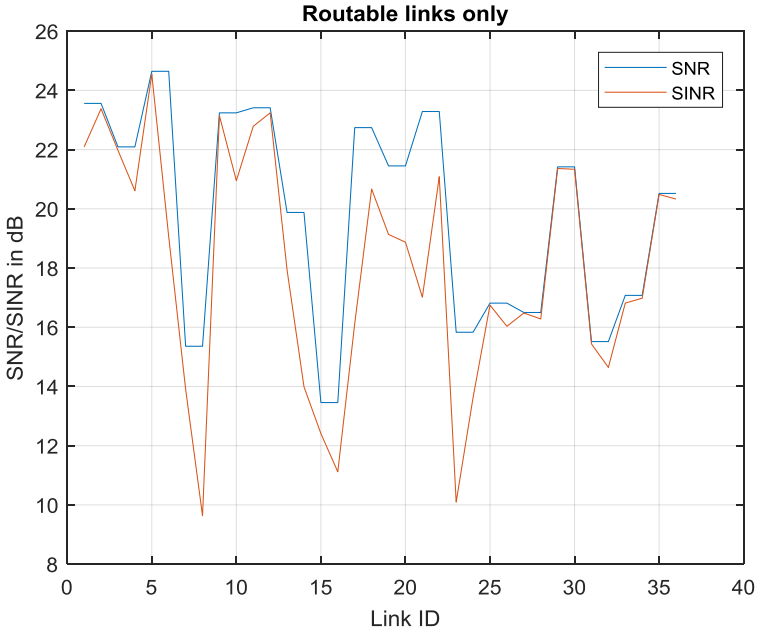

Figure 4-21. SNR and SINR of routable links (reuse3 1 POP).

The reuse=3 network plan ensures that the interference levels are low, as evident by the high SINR values, Figure 4-21. There are three routable links at MCS10, one at MCS11, and the remaining 32 use MCS12.

With the single POP, the BH rates per node are limited by the aggregation of traffic which culminates with the final hop to the POP. An offered load of 75 Mbps uplink and 250 Mbps downstream was found to be sustainable (no continuous buffer accumulation). Results are captured in Figure 4-22, Figure 4-23 and Figure 4-24. Again, the mean latency is roughly 0.5 ms per hop, with the maximum latency only slightly higher.

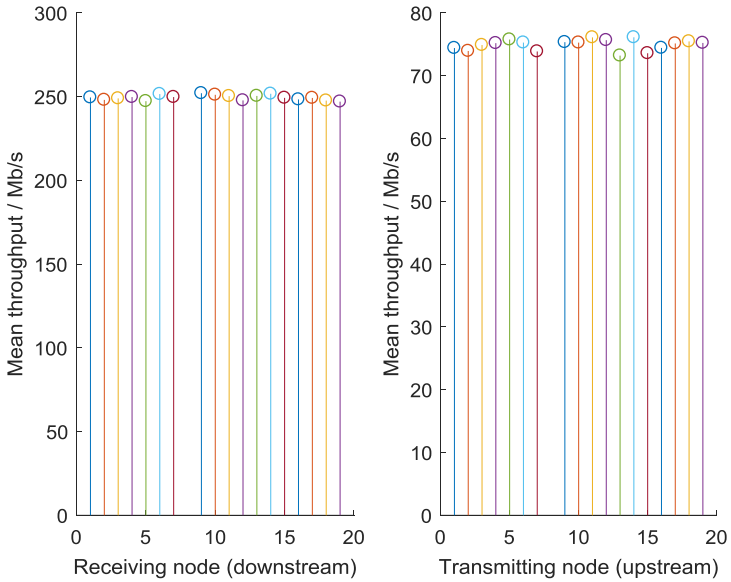

Figure 4-22. Throughput per node (reuse3, 1 POP).

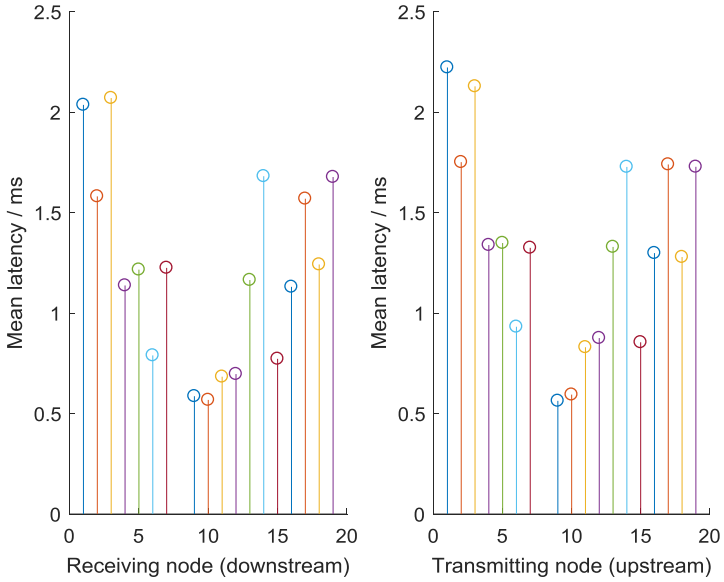

Figure 4-23. Mean latency per node (reuse3, 1 POP).

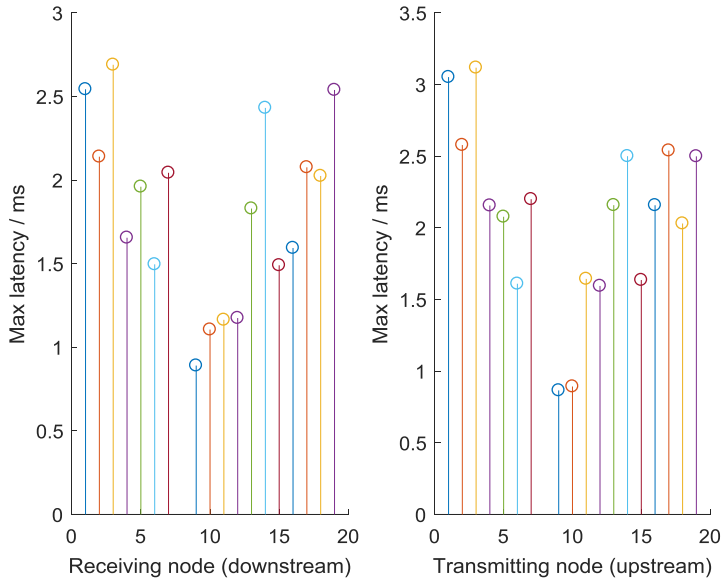

Figure 4-24. Max latency per node (reuse3, 1 POP).

Finally, Figure 4-25 compares the offered load values for the three scenarios, and Figure 4-26 compares the mean (mean latency per pkt per node) values. It is clear that the deployment of more POPs and using more channels increases the achievable BH rates. The latency depends largely on the number of hops, soit is driven by the number of POPs deployed rather than the number of channels used.

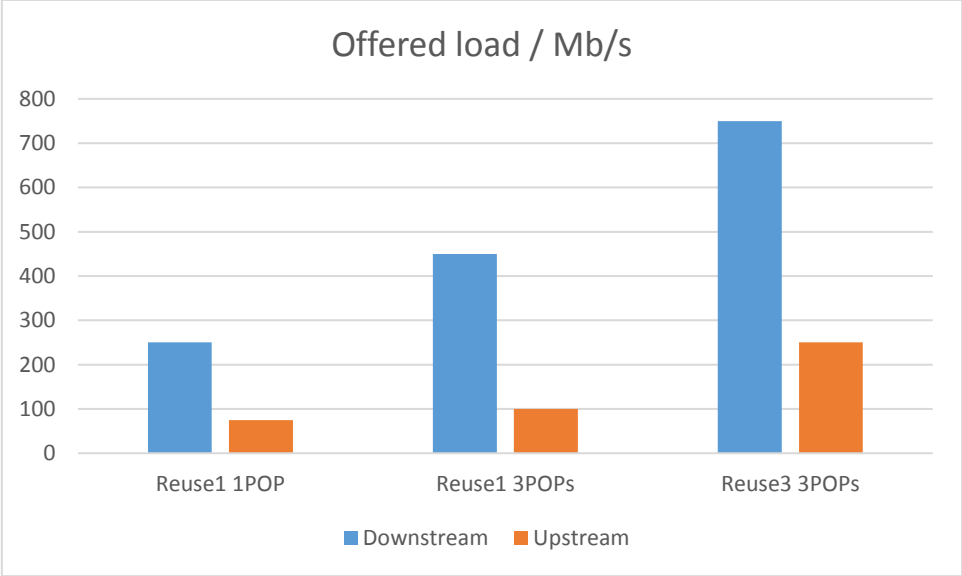

Figure 4-25. Comparative traffic load per node for dynamic simulations.

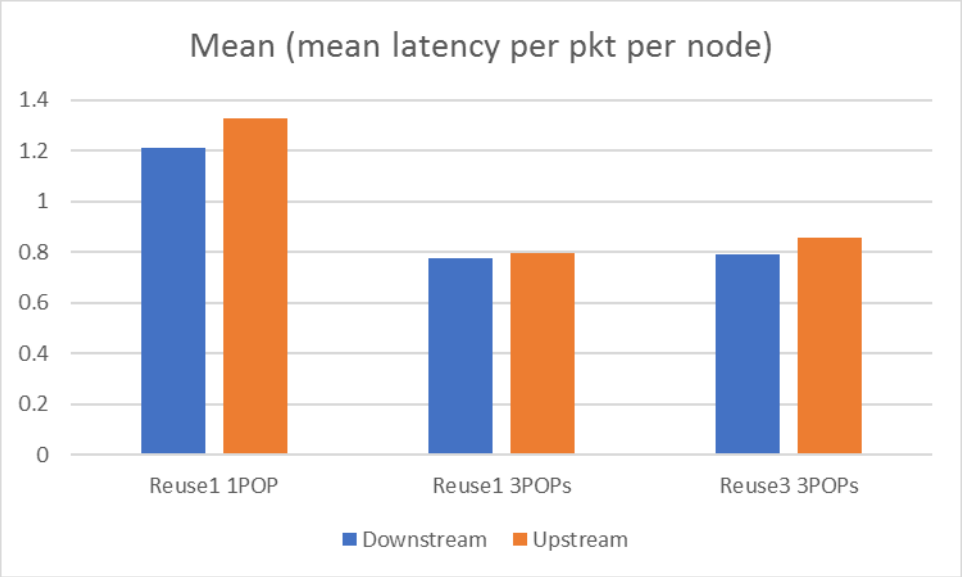

Figure 4-26. Mean (mean latency per pkt per node) in ms.

5 Summary and Conclusions

This report has undertaken new work to assess:

- the usefulness of mmWave technologies for FH,
- the joint design of access and BH in the mmWave band, and
- the BH performance of meshed mmWave links using a dynamic system simulator.

The latest mmWave technology is typified by IEEE 802.11ay which promises useful link rates of 27.5 Gbps with the bonding of 4 channels. Higher rates (x4 or x8 of this value) are possible under environmental conditions that permit the use of multiple stream MIMO. In outdoor deployments these are unlikely to be common, however. Using the conservative rate quoted, the mmWave technology can support the bandwidth needs of fronthaul with low level functional splits for LTE. For future higher capacity small cells a high functional split split C is recommended. The latency performance of IEEE 802.11ad/ay is constrained by the duplex scheme (TDD) and the overhead from common channels. This also points towards FH with higher functional splits where latency requirements are more relaxed. The introduction of multiple hops will make fronthaul more difficult because the bandwidth per RRU tends to fall because of traffic concentration, and the latency increases.

The design of a joint radio access and FH receiver is summarised (more detail is found in [16] and [17]). The performance gain at the link level is approximately 2 dB in SNR when the FH is unreliable, for example, when it is raining. However, there is no gain in the absence of rain.

The advantages of wireless self-backhauling have been outlined. In this scheme the access and BH share the same wireless channel. In the mmWave band beamforming can be used to isolate access and BH links, thus enabling full sharing of the wireless band. When isolation is not sufficient sharing in time or frequency must be used.

A dynamic system simulator has been used to evaluate the performance of a mmWave meshed BH network deployment in the *Eixample* quarter of Barcelona. The IEEE 802.11ad technology at 60 GHz is assumed. The simulator estimates path and antenna gains between nodes, designs PBSSs including channel assignment, calculates routes and then sends packets over the mesh from small cells to fibre POPs. Even with a single channel it is possible to BH all the small cells. The latency is approximately 0.5 ms per hop. The deployment of more POPs and using more channels increases the achievable BH rates. The latency depends largely on the number of hops, so is driven by the number of POPs deployed rather than the number of channels used.

6 REFERENCES

[1] 5G-XHaul, Deliverable D4.9, “Initial Report on mm-Wave Circuits and Systems for High Rate Point to Multipoint Links”, December 2016.

[2] 5G-XHaul, Deliverable D4.4, “Advanced signal processing techniques for capacity improvement in the wireless domain”, June 2017.

[3] 5G-XHaul, Deliverable D4.5, “Extended 60 GHz Matlab simulator and incorporation of new algorithms”, Sept 2016.

[4] 5G-XHaul, Deliverable D4.6, “Real time implementation of advanced MIMO algorithms in BWT DP1 platform”, Sept 2016.

[5] 5G-XHaul, Deliverable D4.7, “Test results from field trial, real time algorithms in BWT DP1 platform”, December 2016.

[6] 5G-XHaul, Deliverable D4.8, “D4.8 Report detailed performance conclusions and system design recommendations”, June 2017.

[7] DragonWave Inc. “Harmony Eband Product Sheet”, Product Sheet, 2016. , [Online]. Available: http://www.dragonwaveinc.com/system/files/bro-000001-05-en_harmony_eband_product_sheet.pdf. Accessed Aug. 18, 2017.

[8] IEEE, “Part 11: Wireless LAN Medium Access Control (MAC) and Physical Layer (PHY) Specifications”, IEEE 802.11-2016.

[9] IEEE, “Draft Standard for Information Technology – Telecommunications and Information Exchange Between Systems – Local and Metropolitan Area Networks – Specific Requirements – Part 11: Wireless LAN Medium Access Control (MAC) and Physical Layer (PHY) Specifications –Amendment 7: Enhanced throughput for operation in license-exempt bands above 45 GHz”, IEEE P802.11ay/D0.35, May 2017.

[10] iJOIN, Deliverable D2.3 – “Final definition and evaluation of PHY layer approaches for RANaaS and joint backhaul-access delay”, April 2015.

[11] 5G-XHaul, Deliverable D2.1 – “Requirements Specifications and KPIs Document”, November 2015, [Online]. Available: http://www.5g-xhaul-project.eu/download/5G-XHaul_D_21.pdf. Accessed Aug. 18, 2017.

[12] 5G-XHaul, Deliverable D2.2 – “System Architecture Definition”, July 2016, [Online]. Available: http://www.5g-xhaul-project.eu/download/5G-XHaul_D2_2.pdf, Accessed Aug. 18, 2017.

[13] 5G-XHaul, Deliverable D2.3 – “Architecture of Optical/Wireless Backhaul and Fronthaul and Evaluation”, December 2016.

[14] 5G-XHaul, Deliverable D3.1, “Analysis of state of the art on scalable control plane design and techniques for user mobility awareness. Definition of 5G-XHaul control plane requirements”, July 2016

[15] J. Bartelt, et al. "5G transport network requirements for the next generation fronthaul interface." *EURASIP Journal on Wireless* Communications *and Networking,* vol. 1, no. 89, 2017

[16] J. Bartelt, D. Zhang, and G. Fettweis, “Joint Uplink Radio Access and Fronthaul Reception Using MMSE Estimation”, *IEEE Transactions on Communications*, accepted for publication, 2017.

[17] J. Bartelt, “Joint Design of Access and Fronthaul Uplinks in Cloud Radio Access Networks”, PhD Thesis, TU Dresden, 2017.

[18] P. Chanclou, A. Pizzinat, F. L. Clech, et al., ”Optical fiber solution for mobile fronthaul to achieve cloud radio access network“, *Future Network and Mobile Summit (FuNeMS) 2013*, Jul. 2013, pp. 1–11.

[19] ITU, ITU Recommendation ITU-R P.837-6: *“*Characteristics of precipitation for propagation modeling*”*, ITU-R, Feb. 2012.

[20] 5G-XHaul, Deliverable D4.13, “Synchronization and localization for cooperative communications”, March 2017.

[21] C.C. Chen, “Attenuation of electromagnetic radiation by haze, fog, clouds and rain”, US Air Force Project RAND, April 1975, http://www.dtic.mil/dtic/tr/fulltext/u2/a011642.pdf.

[22] 5G-XHaul, Deliverable D2.4, “Network Topology Definition”, Jan 2017.

[23] 3GPP Technical Specification Group Services and System Aspects; 22.261 v16.1.0 (2017-09).

7 ACRONYMS

Acronym	Description
ACK	Acknowledgement
AFE	Analog front end
AMC	Adaptive Modulation and Coding
BER	Bit error rate
BH	Backhaul
CPRI	Common Public Radio Interface
CU	Centralised Unit
eNB	Evolved Node B
EPC	Evolved Packet Core
FH	Fronthaul
HARQ	Hybrid Automatic Repeat ReQuest
IMIX	Internet traffic mix
KPI	Key Performance Indicator
LOS	Line-of-sight
MAC	Medium Access Control
MCS	Modulation and Coding Scheme
MIMO	Multiple Input Multiple Output
MMSE	Minimum Mean Squared Error
mmWave	Millimetre Wave
MPDU	MAC protocol data unit
NGCN	Next generation core network
NLOS	Non Line-of-sight
OFDM	Orthogonal Frequency Division Multiplexing
PBSS	Personal Basic Service Set
PCP	PBSS Control Point
PHY	Physical layer
POP	Point of presence
QoS	Quality of Service
RACH	Random access channel
RAN	Radio Access Network
RRH	Remote Radio Head
SINR	Signal to interference plus noise ratio
SNR	Signal to noise ratio
STA	Station
SyncE	Synchronous Ethernet